This is to certify that the

thesis entitled

EXPERIMENTAL AND NUMERICAL TECHNIQUES RELATED TO

THE MAXIMUM ALLOWABLE DEPTH OF APPLES IN A

BULK STORAGE

presented by

YOOSEF SHAHABASI

has been accepted towards fulfillment
of the requirements for

~~Ph.D.~~ degree in ~~Agr. Eng.~~

Larry J Segerlind
Major professor

Date Feb. 22, 1980

EXPERIMENTAL AND NUMERICAL TECHNIQUES RELATED TO THE MAXIMUM ALLOWABLE DEPTH OF APPLES IN A BULK STORAGE

By

Yoosef Shahabasi

A DISSERTATION

Submitted to
Michigan State University
in partial fulfillment of the requirements
for the degree of

DOCTOR OF PHILOSOPHY

Department of Agricultural Engineering

1979

ABSTRACT

EXPERIMENTAL AND NUMERICAL TECHNIQUES RELATED TO THE MAXIMUM ALLOWABLE DEPTH OF APPLES IN A BULK STORAGE

By

Yoosef Shahabasi

The objective of this study was to develop experimental and analytical techniques to determine the maximum safe depth for apples in a bulk storage. The problem was perceived to consist of two components. One component involved the determination of the contact forces in a bulk bin while the other component related to the determination of whether a specific loading would produce a bruise.

The mechanical properties of Jonathan apples before storage and two periods during storage were determined experimentally by compressing cylindrical specimens until a failure occurred. The modules of elasticity changed significantly between October 1 and November 15. A very small change occurred between November 15 and December 31, 1978. The respective averages were E_{OCT} = 3279 Kpa, E_{NOV} = 2516 Kpa and E_{DEC} = 2360 Kpa. The

average maximum normal strain at failure was 0.14, 0.11 and 0.12 for three dates. The average normal stress at failure decreased from 444 Kpa on October 1 to 252 Kpa on November 15 and 235 Kpa on December 31. One hundred fifty apples were sampled on each date with four samples being removed from each apple.

The distributions of the elastic modulus and failure strain were used in a computer model to predict bruising for a particular load. The model was based on the assumption that a bruise occurs when the maximum normal strain exceeds a specified value. The load which produced a bruise was converted to a depth by assuming a single column stack for the apples.

Apple-to-apple contact was found to govern the allowable depth. The October 1 apples could be piled 5.14 meters without brusing but the November 15 and December 31 apples could be piled only about 1.8 meters. The significant decrease was attributed to the decrease in the modulus of elasticity between October 1 and November 15.

As existing finite element type computer model which had been used to model the contact forces between small diameter steel balls was modified for use with large diameter low modulus materials such as apples. The validity of the model was established by experimentally measuring the contact forces between 6 cm diameter rubber

balls which were stacked in a rhombohedral fashion. There were seven layers with either four or five balls in each horizontal layer. All of the contact forces differed by less than 20 percent from the values calculated using the computer model.

Approved: Larry Segerlind
Major Professor

Richard H. [illegible]
Department Chairman

To Sattar

and

Masumeh

ACKNOWLDGEMENTS

The author sincerely appreciates the guidance and cooperation of his major professor, Dr. Larry J. Segerlind (Agricultural Engineering) during the development of this research work. Also appreciation is extended to Dr. Haruhiko Murase (Agricultural Engineering) for his helpful suggestions. Equally, his gratitude is extended to Dr. D. H. Dewey (Horticulture), Dr. W. N. Sharpe, Dr. G. E. Mase (Metallurgy, Mechanics and Material Science), Dr. G. K. Brown (USDA) and Dr. R. H. Wilkinson (Agricultural Engineering).

Thanks are due to his parents, brothers, sister and uncle for their encouragement throughout this study.

The author is particularly indebited to the Iranian people from which, through a scholarship, this graduate work was made possible.

TABLE OF CONTENTS

LIST OF TABLES

LIST OF FIGURES

Figure		Page

Figure		Page

Figure		Page

LIST OF APPENDICES

I. INTRODUCTION

Apples utilized by the processing industry are usually stored in stacks of bulk bins in the plant yard. Apples received early in the harvest season are subjected to moderate daily temperatures that hastens ripening which increases the shrink due to weight loss and spoilage. Apples harvested late in the season may suffer from freezing damage around the stacks despite some protection from straw or plastic covering.

Cold storage is being used with increasing frequency despite its cost, particularly by slice processors. The higher cost of storage and a trend to fewer and larger plants necessitates reducing the overhead by operating the plant for a longer period. One method of reducing the overhead is to construct less expensive types of storage which will protect the apples from excessive heat or freezing conditions.

The USDA agricultural research group at Michigan State University have been developing a totally integrated system of equipment for mechanically harvesting, transporting, and storing apples. A description of the bulk storage silo and the procedure for its loading and unloading has been reported by Burton and Tennes (1977), and Tennes, et al. (1978). The system consists of:

a. A quick acting mechanical shaker designed to shake the trunks of trees spaced as close as 2.4 meters (8 feet) apart, while moving at 1.6 Km/h (1 mile/h).

b. A horizontally positioned reinforced fiber glass tank mounted on a heavy duty trailer with a filling-well at the top center of the tank. The tank holds 8300 liters of water and is used to transport the apples, Figure 1.1.

c. A bulk silo storage system consisting of a storage facility, a reservoir that can provide a large amount of water and a conveyer and handling apparatus for the loading and unloading of fruit from the storage, Figure 1.2.

Recommended management practices for bulk storage includes the avoidance of loading warm fruit into the storage (this can be done by hydrocooling of fruits before storage) and controlling the temperature during storage by proper insulation and ventilation using cool night air. The depth of apples should also be such that little bruising occurs within the stack. The determination of the maximum safe depth for apples stored in bulk is a factor that has not been determined. A study of the

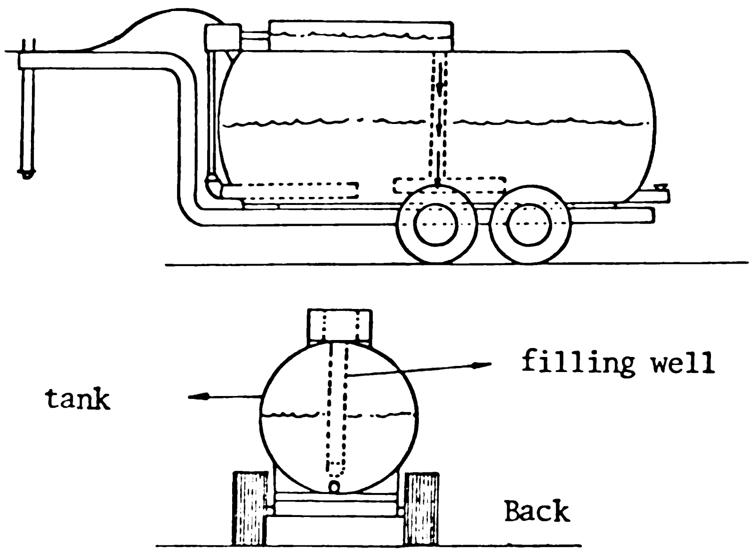

Figure 1.1 View of the Handling Tank System with a Conventional Apple Harvester.

loads acting on apples and the allowable depth for safe storage is needed.

The primary objective of this study was to develop some experimental and analytical techniques in determining the maximum depth for safe storage of Jonathan apples in a bulk bin. Specific objectives were:

1. To study the changes in the mechanical properties of Jonathan apples during refrigerated storage and use these in a simulation model to predict the allowable storage depth.
2. To study the contact force distribution and transmission in the bulk storage of large diameter spheres.

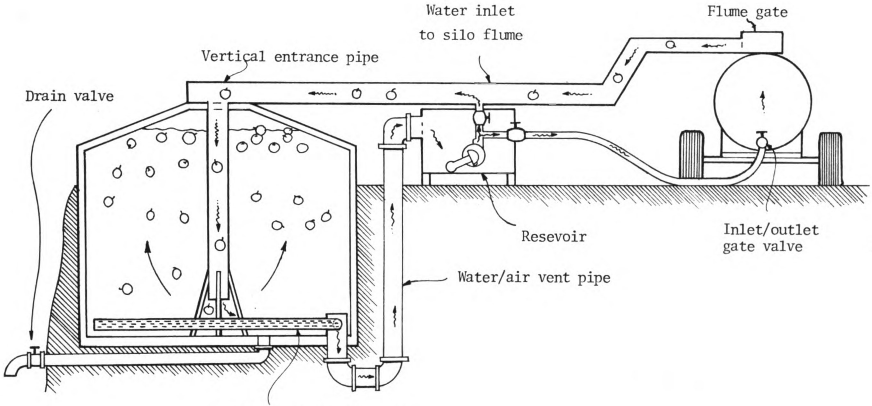

Figure 1.2.--Silo Storage Being Filled (Tennes, 1977).

II. REVIEW OF LITERATURE

2.1 Mechanical Injury

Bruising and injury to agricultural commodities during mechanical handling operations has been a problem of interest to agricultural engineers for several years. As a result, many investigations have been conducted to determine the mechanical behavior of agricultural products when they were subjected to various types of external forces. The increase in use of mechanical harvesting for agricultural products has generated a need for basic information on material properties.

Gaston and Levin (1951) reported an extensive study of causes of apple bruising in handling operations. Their study included the loading of apples under both impact and dead load conditions. For the impact test, apple samples were dropped from heights up to 24 inches onto various types of surfaces. Apples were subjected to an increasing dead load until the desired load of bruising has been achieved. They reported that a dead load of 8.5 pounds was required to produce a 3/8 inch diameter bruise in a 2.5 inch diameter McIntosh apple. No bruise occurred below 8.5 pounds. Above this load, the amount of bruising was proportional to the load applied. Their test included a very large number of apple samples and the data reported were aimed more toward demonstrating the importance of minimizing loads on apples.

Mohsenin and Göhlich (1962) carried out a more intensive study to determine some of the important engineering parameters involved in mechanical damage. They studied apple sections under impact and static loads. The static test was conducted by applying various dead loads on the apples for 100 hours at 34°F. The energy required to bruise under an impact load was found to be roughly twice that required under a static load.

Fletcher et al. (1965) studied the effect of variable loading rates to determine trends of the rate characteristics, rather than the properties at isolated rates of loading. They wanted to correlate the mechanical properties at one rate of loading with those at another. Their study brought out some important relationships between slow and fast rates of loading but they did not investigate maximum allowable loads.

Hammerle and Mohsenin (1966) used a vertical drop tester for dynamic impact loading. The main objective of their study was to develop the apparatus and the method of testing.

Bittner et al. (1967) developed the concept of using a simple pendulum to simulate free fall of the fruit specimens. They used the energy balance theory to evaluate the effectiveness of various cushioning materials based on rebound energy, energy absorbed by the cushion and energy absorbed by the apple.

Fridley and Adrian (1966) worked on resistance to mechanical injuries of apples. Their results, given in terms of compression yield force and impact yield energy, showed that in comparison with peaches, pears and apricots, apples had the least potential for mechanical harvesting.

Mattus et al. (1960) showed that drop heights more than six inches onto a hard surface produces internal bruise in pears which developed brown spots in the flesh of the fruit.

Location of the bruise has suggested that maximum shear stress can be a possible failure parameter (Fridley and Adrian, 1966). A dynamic triaxial compression test was conducted by Miles and Rehkugler (1971) at varying levels of compression stress, shear stress and axial strain rates. These investigators reported that shear stress was the most significant failure parameter.

Dal Fabbro (1979) concluded that the maximum normal strain is the primary factor causing the failure of apple flesh.

2.2 Stress Analysis in Fruits Under Loading

Knowledge of the stress distribution in fruits under static and impact load is limited because of the difficulty involved in determining material properties and the lack of analytical solutions valid for the irregular shapes involved. The load could be exerted from a flat body to the fruits or from one fruit to another.

Finney (1963) reported a significant difference existing between certain potato varieties in their response to applied surface pressure. Mohsenin and Gölich (1962) applied the same technique to apples, potatoes, pears and tomatoes concluding that the compression test appeared to offer the most promise of evaluation of mechanical behavior as related to bruising.

The most common type of loading that fruits are subjected to is the contact load which can produce a bruise. Contact forces occur in harvesting, handling and storage. Contact stresses are caused by the pressure of two bodies having a point (small area) contact: common type of contacts are the sphere and a plane, Figure 2.1 or two spheres, Figure 2.2. Boussineq (1885) solved the problem of concentrated forces acting on the boundary of a semi-infinite body. Timoshenko and Goodier (1970) discuss the contact problem as solved by Hertz. The maximum

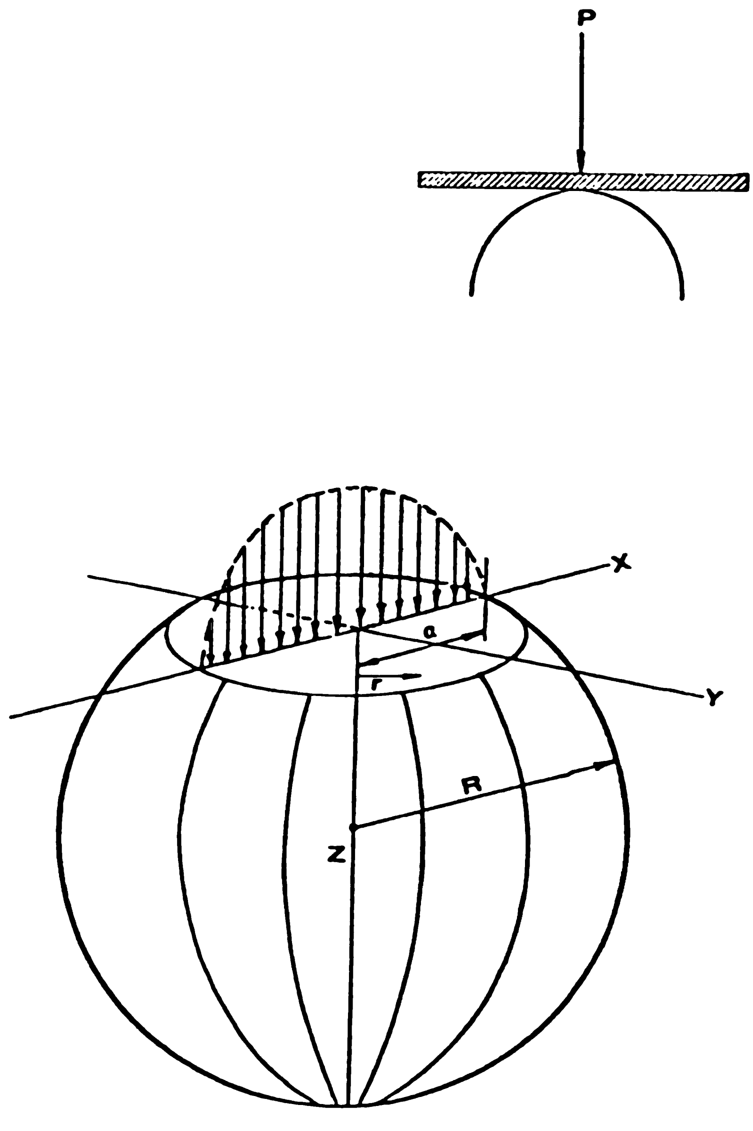

Figure 2.1.--Pressure Distribution on the Contact Surface of Sphere as Subjected to a Flat Plate Under Load.

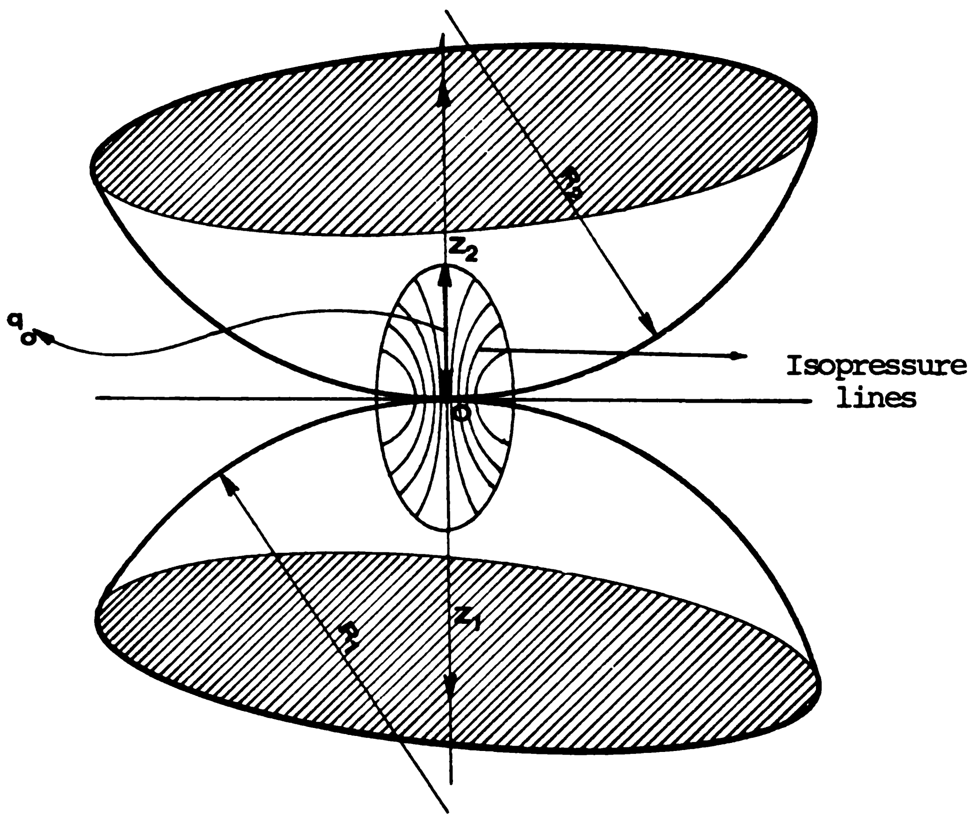

Figure 2.2.--Hertz Theory of Contact for Two Spherical Bodies in Contact.

pressure on two spherical bodies in contact is 1.5 times the average pressure on the surface of contact or

$$q_o = \frac{3P}{2\pi a^2} \tag{2.1}$$

Assuming that both balls have the same elastic properties and taking $\mu = 0.3$ the corresponding maximum pressure is

$$q_o = 3/2\ \frac{P}{\pi a^2} = 0.388\ \sqrt[3]{PE^2\ \frac{(R_1 + R_2)^2}{R_1^2 \cdot R_2^2}} \tag{2.2}$$

where q_o is maximum pressure on the surface of contact

a is the radius of the surface of contact

P is the applied load

E is the modulus of elasticity of spheres

R_1 is the radius of sphere one

R_2 is the radius of sphere two

The first known application of Hertz solution for contact stresses in agricultural products is reported by Shpolyanskaya (1952) for determination of modulus of deformability of the wheat grain compressed between two parallel plates.

Finney (1963) used the Boussinesq solution for concentrated forces acting through a rigid die for potato, apple, portions of corn kernels, peaches and pears. The

Hertz and Boussinesq techniques have also been applied to apples (Morrow and Mohsenin, 1966). McIntosh apples were subjected to constant load (creep test) or constant deformation (stress relation test) by a flat rigid plate. In the case of McIntosh apples loaded with a 1/8 inch cylindrical rigid die, they concluded that the stress was approximately zero at a depth of two inches below the surface of the fruit.

Fridley, et al., (1968) applied Hertz and Boussinesq theories to obtain force-deformation curves for peaches, pears and apples. They showed that the bruise in an apple usually occurs under the center of the area of contact at a small distance beneath the surface of the fruit. A flat plate loading was used in the study.

Agricultural products are generally viscoelastic. Viscoelasticity comprises an irreversible energy transformation where the relation between stress and strain is governed by time effect. During the early experiments on mechanical behavior of fruits and vegetables, it was observed that force deformation relations includes the time effect (Finney, 1963; Mohsenin, 1963; Timbers et al., 1966). Experiments conducted on McIntosh apples showed that apple flesh behaves as alinear viscoelastic material (Morrow and Mohsenin, 1966). Latter Chappell and Hamann (1970) studied the viscoelastic behavior of apple flesh, but they found the material properties to be somewhat stress dependent and thus could not be characterized as linear. Hamann (1967 and 1970) also noted the nonlinear properties in apple flesh but he solved the apple impact problem for stress at the surface and in the interior of the apple considering apple flesh as a linear-viscoelastic material. In the later studies, the finite element method was used to determine stresses in apples resulting from contact with a flat plate.

Apaclla (1973) considered the apple as an elastic material and used the finite element method. Rumsey and Fridley (1974) used the finite element method assuming a linear viscoelastic shear modulus and an elastic bulk modulus for the material. De Baerdemaeker (1975) considered a material with time dependent bulk modulus and shear modulus to obtain the creep deformation and the stress distribution of a sphere in a contact with a flat rigid plate using the finite element method. He concluded that apples subjected to contact creep loads experience maximum stresses at the initial application of the force. Sherif (1976) solved the quasi-static contact problem for nearly incompressible agricultural products using finite element method.

Other theoretical studies involving vegetative materials includes Gustofson (1974) who obtained a numerical solution to the axisymmetric boundary value problem for a gas-solid-liquid medium and Murase (1977) who developed stress-strain constitutive equations containing parameters necessary to describe the mechanical behavior of vegetative material including the water potential term.

2.3 Criteria for Maximum Allowable Load

One of the major reasons for studying the mechanical properties of fruits and vegetables has been to determine the maximum allowable load to which these materials can be subjected without causing objectionable damage.

Limited work has been done to understand the mechanics of bruising in fruits and vegetables. A recent work using a compression test on tissue specimens reported that shear stress is the most important failure parameter (Miles, 1971). The question of how the maximum allowable shear stress can be determined for a whole fruit was not answered in this work. The concept of "Bioyield Point," indicating initial cell rupture in whole fruits such as apples and pears, has been proposed as the criterion for maximum allowable load that fruit can sustain without showing any visible surface bruising (Mohsenin, 1962 and 1965). In the case of apples the bruise is immediately below the skin and in most cases can be removed in the peeling process. In fruits such as peaches, bruising and tissue failure can occur some distance below the skin and the damaged protion can be seen only in canned products by the consumers. In these cases, shear strength has been taken as the maximum allowable load (Horsfield, 1970).

In recent studies the application of the theory of elasticity and importance of the modulus of elasticity of the fruit in single and multiple impacts suggested that the failure was due to excessive internal shear stresses. It is shown that maximum shear stress is proportional to (a) the energy of fall, (b) the moduli of elasticity of the fruit, and (c) the radii of the fruit and the impact surface (Horsfield, 1970). Nelson and Mohsenin (1968) have determined a relation between bruise volume and load. They report that bruises caused by dynamic loads are larger than those caused by equivalent quasi-static loads. Fletcher et al. (1965) reported that energy force and deformation to repture first decreases with increasing loading rate, then increases. Mohsenin (1971) reported that, the significance of certain viscoelastic properties of fruits and vegetables may not be understood but we should be ready to use such data as the maximum allowable load that these products can sustain under impact, dead loads, and vibration in designing handling systems. He also mentioned that these data should be available in the form which can be used by engineers.

Dal Fabbro (1979) studied the strain failure of apple material. Cylindrical and cubic apple specimens were subjected to uniaxial, biaxial and triaxial state of stress. Linear elastic and viscoelastic material properties were used to calculate the stress and strain components within the apple flesh.

He reported that in the uniaxial loading of cylindrical specimens the normal stress at failure varied for different strain rates. Triaxial loading of cylindrical specimens indicated that maximum shear stress and normal stress at failure vary for different levels of cylindrical stress. He also reported that the uniaxial, biaxial and rigid die loading of cubic and cylindrical specimens discards the maximum normal stress failure criteria.

Experimental results from his studies indicate that the maximum normal strain at failure remains relatively constant for all the loading situations. The most significant conclusion of his research was that apple material fails when the normal strain reaches a critical value.

2.4 Mechanical Properties of Granular Systems

Granular systems consist of cohesionless particles where the individual grains are independent of each other except for frictional interaction and geometric constraints resulting from the particular type of packing. The two most important properties of granular materials are their strength and compressibility characteristics. The component particles in a granular system may be of any size from the smallest diameter of 10μ (like powder) to pebbles, cobbles, or even boulders (several inches in diameter) (Brown, 1970; Farouki, 1964).

Many studies of the packing of solid particles have been based on spherical or near spherical particles. Graton and Fraser (1935) discussed the geometry of various assemblages of discrete, ideal spheres. Also systematic arrangement of spheres in connection with the flow of water through soil was first studied by Slichter (1899).

2.4.1 The Arrangement of the Particles in a Stack

The stacking arrangement of the particles in a mass of material determines the points of contact between the particles and the direction of the normal at contact points; this essentially establishes the force system which acts between the particles.

2.4.1.1 Systematic arrangement of uniform spheres. Ideal spheres may be packed in ordered layers of various types definable by the angle of intersection of the set of rows in the layer. Layers in which sets of rows have angles of intersection of any value between the limiting values of 60° and 90° are possible. Since square and simple rhombic layers (Figure 2.3) represent the limiting types of systematic packing, only these two are considered.

Figure 2.3.--The Angle of Intersection of the Sets of Rows in the Layer.

Three different systems may be formed by stacking square horizontal layers one above another.

Case 1. A simple rectangular system; each sphere has its center vertically above that of the sphere below (Figure 2.4).

Case 2. The orthorhombic system results when the center of the upper sphere is offset a distance R in the direction of one of the rows (R is the radius of the spheres) (Figure 2.5).

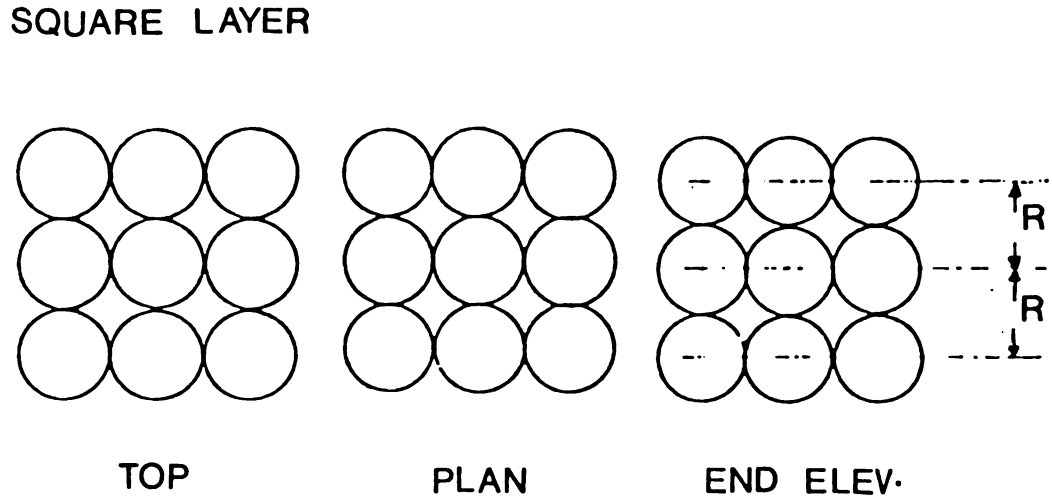

Figure 2.4.--A Simple Rectangular System.

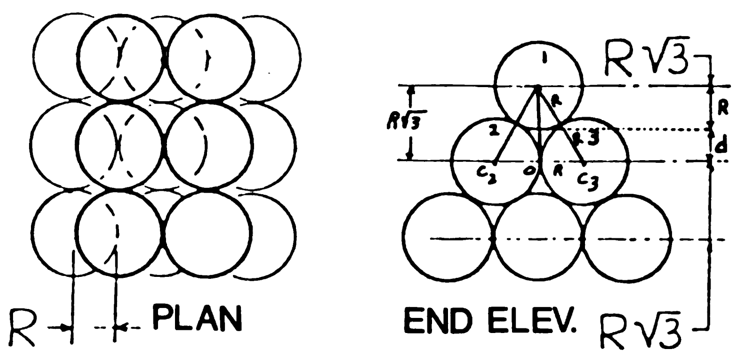

Figure 2.5.--The Orthorhombic System.

To get the vertical distance, d, between the center of a sphere in a row whith the one above or below it, consider triangle $C_1O\,C_3$ (Figure 2.5) which can be written:

$$R^2 + (d + R)^2 = 4R^2$$

$$d^2 + 2dR - 2R^2 = 0$$

$$d = \frac{-2R + 2\sqrt{3}\,R}{2} \text{ or } d = -R + \sqrt{3}\,R = 0.73\,R \quad (2.3)$$

Case 3. Rhombohedral system. In this case each sphere is in contact with four spheres below, four above, and four in the same layer (Figure 2.6).

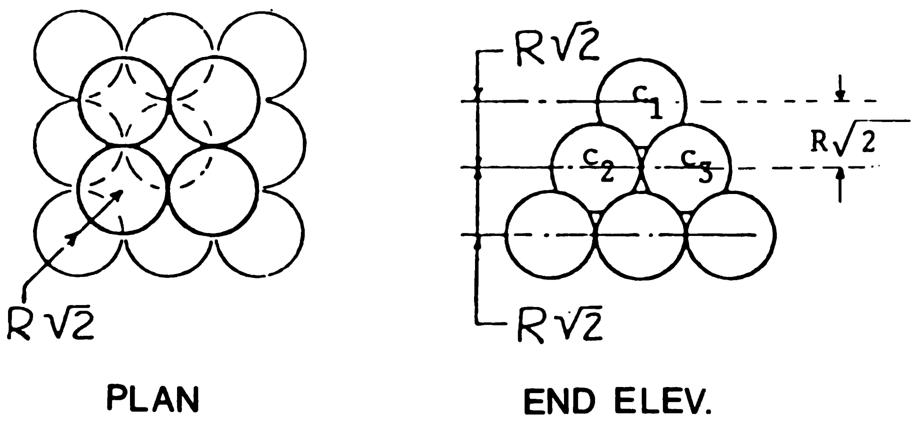

Figure 2.6.--Rhombohedral System.

To get the projectional distance between two spheres in two layers, consider the pyramid of $C_1C_2C_3C_4C_5$ with the trianglar side of $C_1C_3C_5$ (Figure 2.7).

Knowing y in this triangle which is:

$$y^2 = 4R^2 - R^2$$

or

$$y = \sqrt{3}\ R$$

will give x as

$$X^2 = 3R^2 - R \quad \text{or} \quad X = \sqrt{2}\ R \tag{2.4}$$

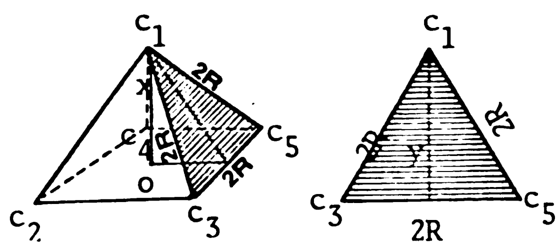

Figure 2.7.--Pyramid and Its Triangler Side.

The rhombohedral system is the most important theoretically, and usually is the basis for calculations. It is also the most important from a practical viewpoint, because it gives the densest state.

The three packing configurations discussed below may be formed by stacking simple rhombic layers one above another.

Case 4. When in the orthorbombic system, the spheres of the next rehombic layer are placed in such a way that the center of each sphere lies vertically above the sphere below it (Figure 2.8).

Case 5. There is a rhombic layer at the bottom and each sphere in the next rhombic layer rests in the cusp between two spheres in the layer below (Figure 2.9).

The distance d is obtained by considering the triangle $C_1C_2C_3$, giving $d = R\sqrt{3}$.

Case 6: This system is similar to case three except each layer from the top is in rhombic form (Figure 2.10).

To find distance d consider pyramid $C_1C_2C_3C_4$, distance y can be calculated by considering triangle $C_4C_3C_2$, then y would be $y = \sqrt{3}\ R$.

Having y, d can be calculated easily from triangle C_4OH as:

$$d^2 = y^2 - \frac{1}{9}y^2 \quad \text{or} \quad d = \frac{2\sqrt{2}\ R}{\sqrt{3}}$$

The angle which the side wall makes with the bottom influences the packing formation (Faruki and Winterkorn, 1964).

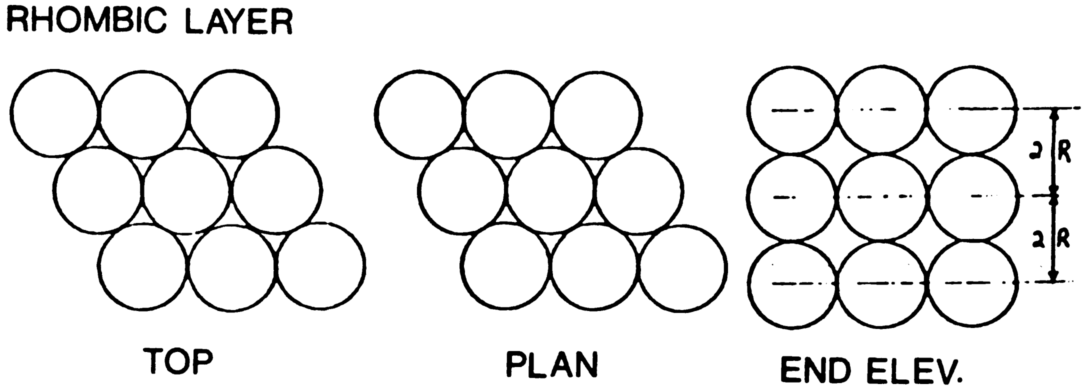

Figure 2.8.--A Rehombic Layer above Another.

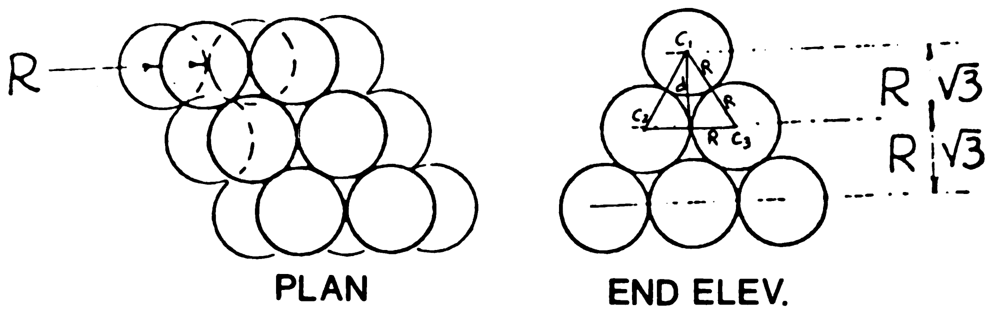

Figure 2.9.--A Rhombic Layer above the Cusp of Another.

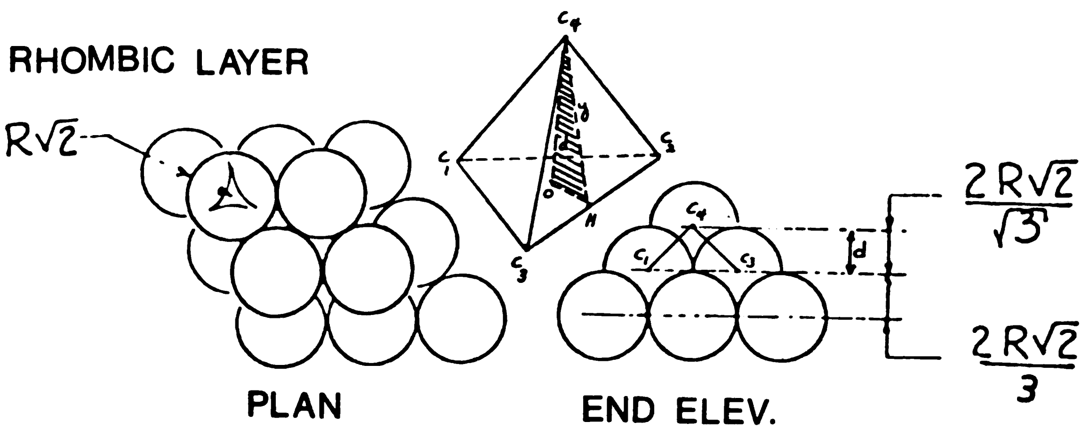

Figure 2.10.--A Rhombohedral System with a Rhombic Form on the Top.

A 90° angle will favor cases 1, 2, 4, and 5, a 60° or 120° angle favors cases 2 and 3. The packing is also influenced by the angel which the side walls make with each other. A 90° angle favors formation of square pattern and hence cases 1, 2, and 3. Intersection of the side walls at 60° with themselves and at 90° with the bottom favors cases 4 and 6.

The walls of the container give rise to a wall effect which causes the porosity in the vicinity of the wall to be greater than that in the body of the packing. This has been studied by Furnas (1929) who obtained an expression for the voids, V_W, present in a ring at the wall of area $\pi d \cdot D/2$

$$V_W = \{V + K\ (1 - V)\}\ (\frac{1 + 2\ Kd}{D}) - \frac{2Kd}{D} \qquad (2.5)$$

where d is the diameter of the particle.

D is the diameter of container.

V is the voids present in the interior.

K is an experimental factor found to be 0.3.

The wall effect increases as the ratio d/D decreases.

2.4.2 Systematic Packing of Spheres of Different Sizes

In 1934 Horsfield calculated the decrease in porosity resulting from the insertion into the voids of the rhimbohedral system of successive spheres just large enough to fill the voids. The spheres filling the concave cube voids are termed secondary spheres, whereas those filling the concave-tetrahedron voids are tertiary spheres. The spheres which are inserted in the largest voids left after the secondary and tertiary spheres are called the quanternary spheres. Table 2.1 shows the type of spheres, their radius and porosity for each sphere.

TABLE 2.1.--Effect on Porosity of Spheres Inserted in Voids of Rhombohedral System (Horsfield, 1934)

Sphere Type	Radius[a]	Number of Spheres	Porosity
Primary	1	1	25.95
Secondary	0.4142	2	20.69
Tertiary	0.2247	2	19.01
Quaternary	0.1766	8	15.74
Quinary	0.1163	8	14.81
Filler	0.000	-	3.84

[a]Primary radius = 1.

It should be noted that it is practically impossible to attain a system packed in such a manner.

Hudson (1949) imagined the voids of the rhombohedral system filled with S spheres of equal radii, r, arranged in cubic symmetry. The densest state was obtained when each concave-cube void contained 21 spheres with $r = 0.1782R$ (in which R is the radius of the primary spheres).

2.5 Contact Theory

Most of the theoretical considerations reported in the soil mechanics literature regarding the effect of particle size in granular systems are based on Hertz's contact theory. Since this theory has also been used to evaluate the stresses in fruits and vegetables, it is appropriate to discuss the primary results of this theory.

There are two types of contacts which can occur between apples, apple-to-apple contact and an apple in contact with a flat surface, Figure 2.11. Hertz's equations are different for these two situations.

Heinrich Hertz (1896) proposed a solution for contact stresses in two elastic isotropic bodies touching each other. He attempted to find answers to such questions as the distribution and magnitude of the surface of pressure, and the approach of the center of the bodies under the pressure.

Hertz started by assuming that the contacting solids are isotropic and linearly elastic, and also that the representative dimensions of the contact area are very

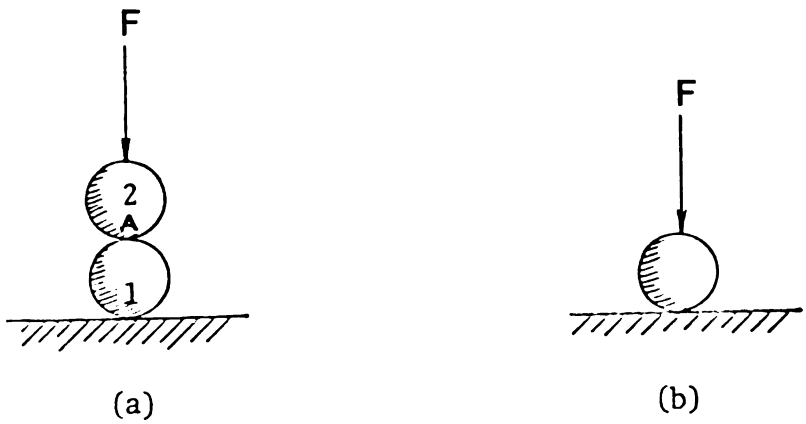

Figure 2.11.--Two Cases of Exerted Load on the Bottom Spheres.

small compared to the radii of curvature of the deformed bodies. This leads naturally to two further simplifying assumptions. Near the contact zone, it is considered sufficiently accurate to represent the actual shape of the two nearly flat bodies by general surfaces of the second degree

$$Z = Ax^2 + By^2 + Hxy \tag{2.6}$$

in which A, B and H are constants depending on the magnitudes of the principal curvature of the surfaces in contact. Hertz also takes the bodies to be "flat" enough, in the neighborhood of the contact surface to be treated by the powerful analytical methods available for the semi-infinite solid, or body bounded by plane. The results obtained by Hertz are summarized below and are found in Shigley (1977).

When two solid circular spheres of diameter D_1 and D_2 are pressed together with a force F, a circular area of contact of radius a is obtained.

Specifying E_1, μ_1, and E_2, μ_2 as the respective elastic constants of the two spheres, the radius a is given by

$$a = \left[\frac{3F}{8} \frac{[(1 - \mu_1^2)/E_1] + [(1 - \mu_2^2)/E_2]}{(1/D_1) + (1/D_2)} \right]^{1/3} \qquad (2.7)$$

The maximum pressure occurs at the center of the contact area and is

$$q_o = -\frac{3F}{2\pi a^2} \qquad (2.8)$$

Equations (2.7) and (2.8) are perfectly general and can be applied to contact with a plane surface by setting either D_1 or D_2 equal to infinity.

The stress components for any point along the Z axis, the axis of symmetry, are

$$\sigma_{rr} = \sigma_{\theta\theta} = q_o \, [-(1 + \mu)[1 - \psi \, \mathrm{Tan}^{-1}(\tfrac{1}{\psi})]$$

$$+ \frac{1}{2}(1 + \psi^2)^{-1}]$$

$$\sigma_{zz} = -q_o\ (1 + \Psi^2)^{-1} \tag{2.9}$$

where $\Psi = z/a$

These normal stress components are the principal stresses since the shear stress components are always zero along an axis of symmetry. The maximum shear stress is given by

$$\tau_{max} = \left|\frac{\sigma_{max} - \sigma_{min}}{2}\right| \tag{2.10}$$

It occurs below the surface and is approximately 0.31 q_o when μ= 0.3. The ratio of the stress components σ_{rr}, $\sigma_{\theta\theta}$, σ_{zz} and τ_{max} to q_o as related to the distance from the surface of contact is shown in Figure 2.12.

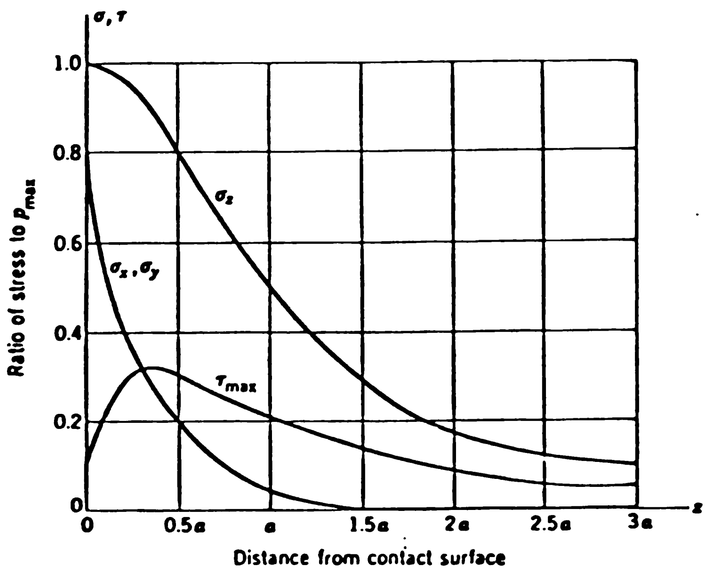

Figure 2.12.--Stress Distribution Within an Elastic Sphere with Poissan's Ratio = 0.3 Compressed with a Flat Plate.

2.6 Contact Forces Between Granular Particles

The load distribution in a granular material has been studied by many people but only a few have suggested equations for determining the contact forces between individual particles. Those studies which appeared to apply to this study are discussed briefly herein.

Ross and Isaacs (1961) formulated a theoretical approach to estimate the forces acting on individual particles in a particle stack. The particles were assumed to be perfect inelastic spheres represented by a certain density and characteristic diameter. They used a simple rhombic stacking model and analyzed the forces acting in such a stack. They generalized equations to predict horizontal and vertical forces on any particle in a stack which were independent of the coefficient of friction of the material, Figures 2.13 and 2.14. They found the total vertical forces exerted by a particle on its support to be

$$F_{tv-n} = \bar{L}_\theta W/\bar{d} \tag{2.11}$$

where $\bar{L}_\theta$ is the average length of the four axis.

W the weight of each particle.

$\bar{d}$ the characteristic diameter.

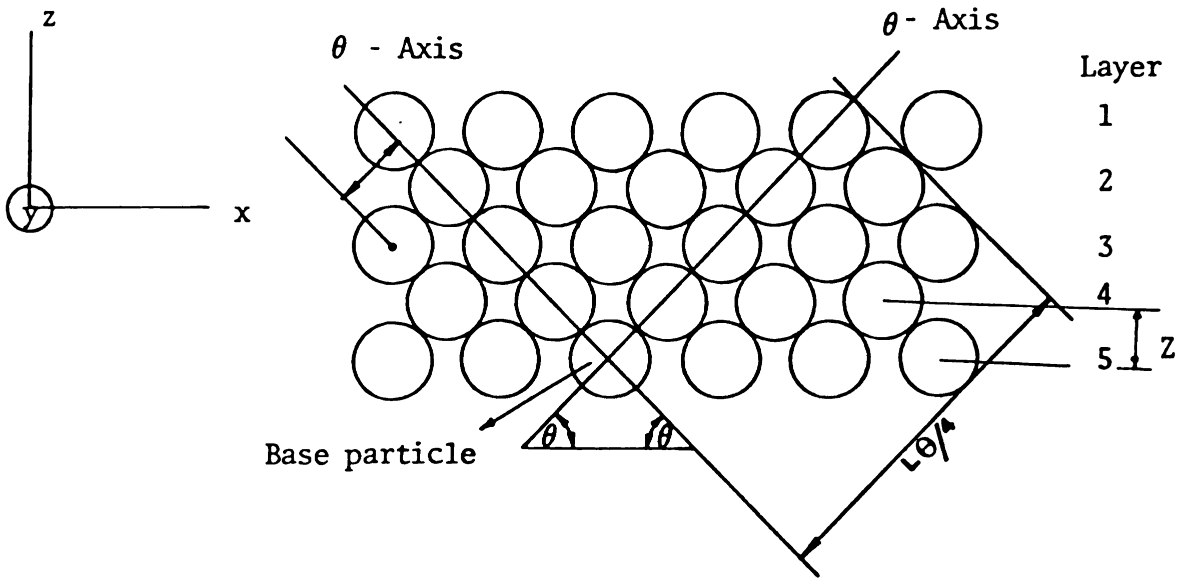

Figure 2.13. Section View of a Model Particle Stack (Ross-Isaccs)

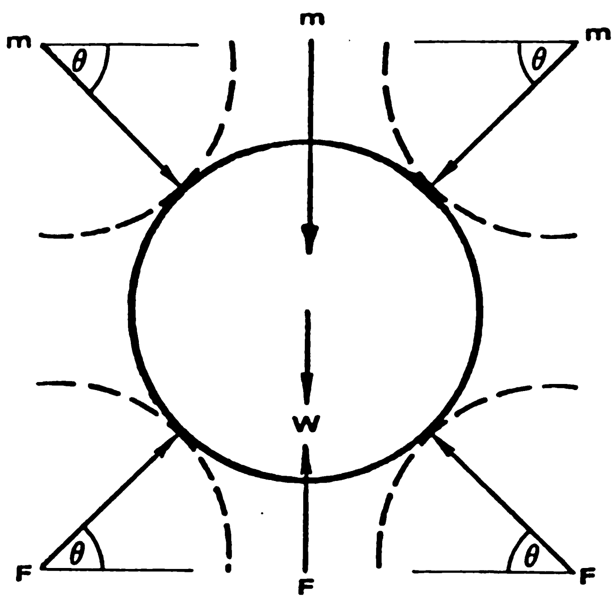

Figure 2.14.- Forces Acting on a Particle in the Particle Stack (Ross-Isaccs)

Marsal (1963) proposed the use of the following semi-empirical equation to calculate the contact forces between the particles:

$$\overline{P} = \left(\frac{\pi r_v \, (1 + e)}{3^{1/4} \, nc}\right)^{2/3} d^2 \, \sigma \qquad (2.12)$$

where r_v is the shape factor.

e is the void ratio.

nc is the average number of contacts per particle.

d is the grain diameter.

σ is the confining pressure.

Keck and Goss (1965) suggested the shape factor as the ratio of geometric mean diameter to the diameter of equivalent sphere.

A study was made by Davis (1974) on the compressibility of and force transmission in a granular material, modeled as a two-dimensional random packing of spheres in elastic contact. He assumed this problem analogous to that of a stochastic planar graph, the nodes of which represent centers of the spheres and the branches, contacts between adjacent spheres. Davis considered the planar graph as an elastic structure and solved the force transmission in a two-dimensional array of randomly packed small steel spheres.

III. ANALYSIS OF THE PROBLEM

The interest in the bulk storage of apples for processing has raised the question of the allowable height to which apples can be piled before causing objectionable damage. The objective of this dissertation is to answer this question.

It has been established by Dal Fabbro (1979) that apple flesh fails when the maximum normal strain exceeds a specific value. The maximum normal strain in a spherical body can be calculated using Hertz's contact theory. This theory shows that the maximum strain is a function of the modulus of elasticity of the body.

There is no reason to believe that the modulus of elasticity of apples remains constant with time. The first part of this study is concerned with determining whether, and if so, how the elastic modulus varies during the storage period. The change in the failure strain and the failure stress must also be studied. Once the distributions of the elastic modulus and failure strain are known, it will be possible to predict whether a force of a specific magnitude will cause a bruise.

The other aspect of the bulk storage problem is the contact force which occurs between the apples. A bulk bin contains too many apples to analyze all of the contact forces even though a computer model for such analysis does exist. This model, however, was developed for small diameter steel balls. The model should be modified to accommodate large diameter, low modulus balls and checked to determine whether it is still valid. The second part of this study is concerned with this modification and check.

IV. CHANGES IN THE MECHANICAL PROPERTIES OF APPLE FLESH DURING COLD STORAGE

4.1 General Remarks

Fruits and vegetables are living organisms which undergo all physiological and pathological processes associated with life. To sustain physiological activities, they draw energy from the food reserves stored within them prior to harvest. This process causes deterioration in the commodities. Deterioration of fresh produce also results from other things, including physiological break down, physical injury to tissue, moisture loss, and invasion by microorganisms. Some, if not all, of these processes can be reduced by placing the produce in a cold storage with proper temperature and humidity conditions. The optimum storage temperature for most varieties is -1°C to 0°C (30°F to 32°F) at 90 percent relative humidity. The normal storage period for the Jonathan variety is two to three months with a miximum of five to six months.

No information is available which shows how the mechanical properties, particularly the elastic modulus and the failure strain, varies with the time period in cold storage. A study to obtian this information is reported in this section.

4.2 Experimental Study

4.2.1 The Test Fruit

Jonathan apples grown during the 1978 harvest season at the Horticultural Farm on the Michigan State University campus were used. The apples were picked on September 29. Eight bushels of 6.35-6.73 cm apples were obtained. Six bushels of these were placed in plastic bags and then in wooden crates and stored in a refrigerated storage. A storage temperature of 1.6-2.2°C (35-36°F) was provided. The other two bushels of apples were taken to the laboratory for immediate testing.

4.2.2 Specimen Preparation

Cylindrical specimens with a height of 1.27 cm (0.5 inch) and a diameter of 1.27 cm and cross-sectional area of 1.266 cm^2 (0.196 in^2) were prepared by driving a corkborer into the apple parallel to the stem calyx axis. The specimen was then put in a cylindrical hole in a plexiglass bar and the ends were cut parallel to the face of the bar by using a sharp blade. All of the apples which were stored at 2.2°C were removed from storage 24 hours prior to testing and allowed to come to room temperature before preparation.

4.2.3 Uniaxial Loading of Cylinderical Specimens

The prepared cylindrical specimens were placed at the center of the load cell of an Instrom TM model testing machine and compressed using a deformation rate of 1.27 cm per minute until a failure occurred. Failure was defined as a discontinuity of the deformation curve as shown in Figure 4.1.

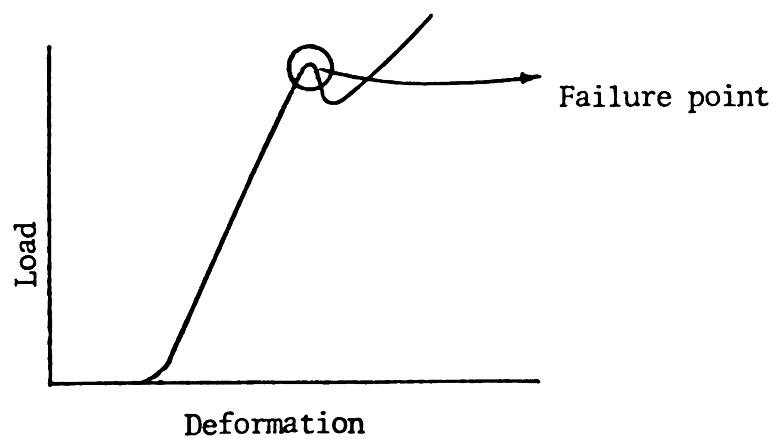

Figure 4.1.--The Failure Point on the Load Deformation Diagram.

Compression tests were performed on three different dates, October 1, November 15 and December 31. These were denoted as Groups I, II and III. Each group consisted of 150 apples and four samples were removed from each apple. The failure strain, ε_f, the stress at failure, σ_f, and the elastic modulus, E, were determined for every sample.

4.3 Experimental Results and Discussion

Tables A1, A2, and A3 of Appendix A give the mean values of the three different parameters (ε_f, σ_f and E) for each of the 150 apples tested for deformation rate on each date. Table 4.1 summarizes the mean value and standard deviation of these parameters for three different groups of Jonathan apples.

TABLE 4.1.--Mean Values and Standard Deviation of the Mean of Three Different Elastic Parameters for 150 Jonathan Apples (1978)

Group	October 1	November 15	December 31
Strain at Failure	0.14 (±0.005)	0.11 (±0.009)	0.12 (±0.008)
Stress at Failure (Kpa)	444 (±30)	252 (±26)	235 (±14)
Modulus of Elasticity (Kpa)	3279 (±260)	2516 (±188)	2360 (±262)

( ) Indicates Standard Deviation of the mean of each apple.

The average modulus of elasticity value for the three storage periods is shown in Figure 4.2. The modulus

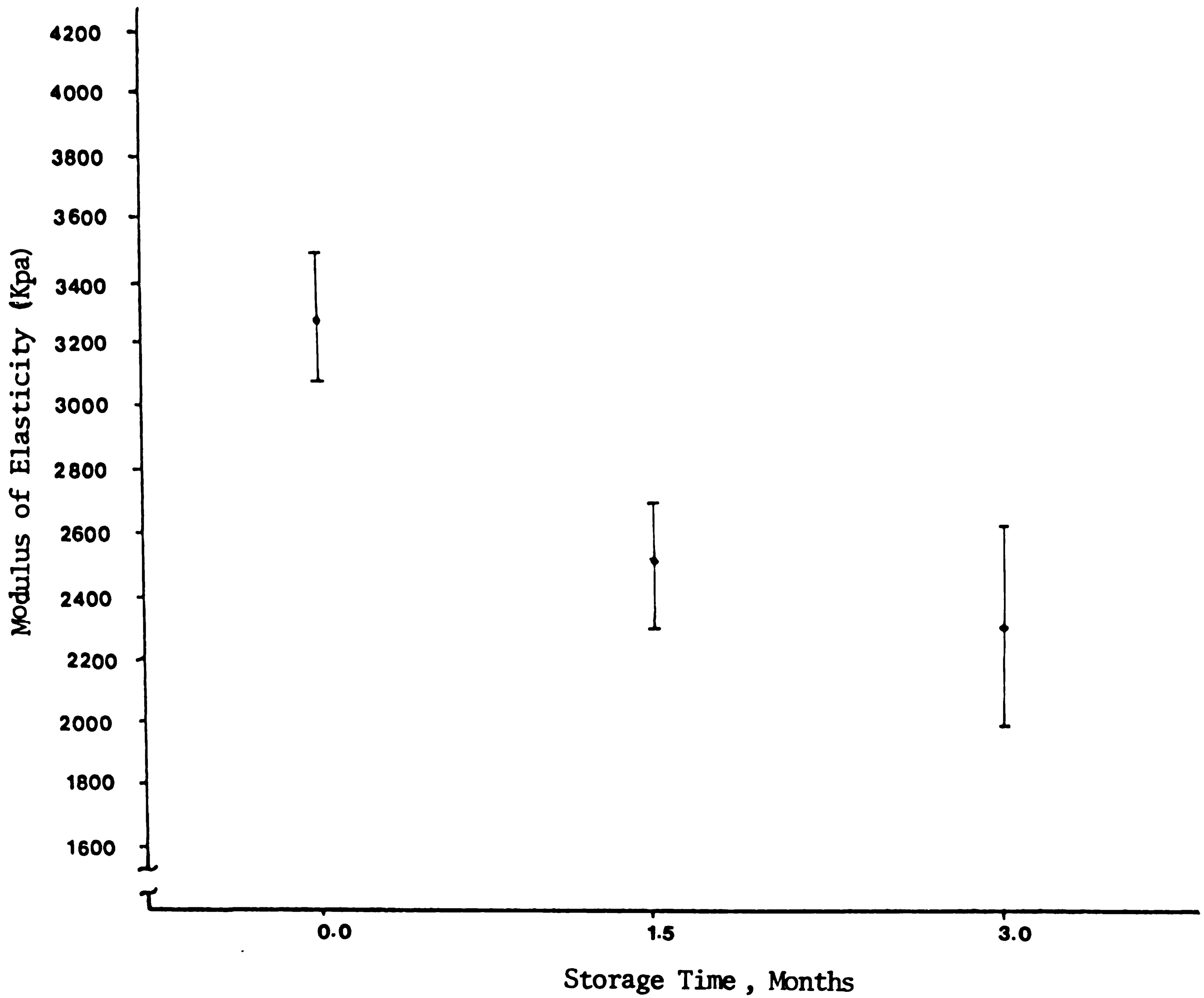

Figure 4.2.-Modulus of Elasticity v.s. Storage Time

of elasticity changed significantly between October 1 and November 15. The decrease in the modulus value was not as much between November 15 and December 31.

Figure 4.3 shows the failure stress had a very sharp decrease in the first 1.5 months, but did not decrease with the same rate for the next 1.5 months.

The failure strain as shown in Figure 4.4 decreased in the first 1.5 months and increased slightly in the next 1.5 months. A statistical investigation (χ^2 test) indicated that the modulus of elasticity and the failure stress depend on the storage period. Failure strain did depend on the storage period for the first 1.5 months but not for the second 1.5 months.

The distribution of the elastic modulus, failure stress and failure strain during the storage period is shown in Figure 4.5 through 4.7. The higher modulus of elasticity and the higher failure strain values for the freshly picked apples indicates a higher resistance to bruising. The changing of the modulus and failure strain values toward smaller values as storage time increases shows a lower resistance of apple material to bruising.

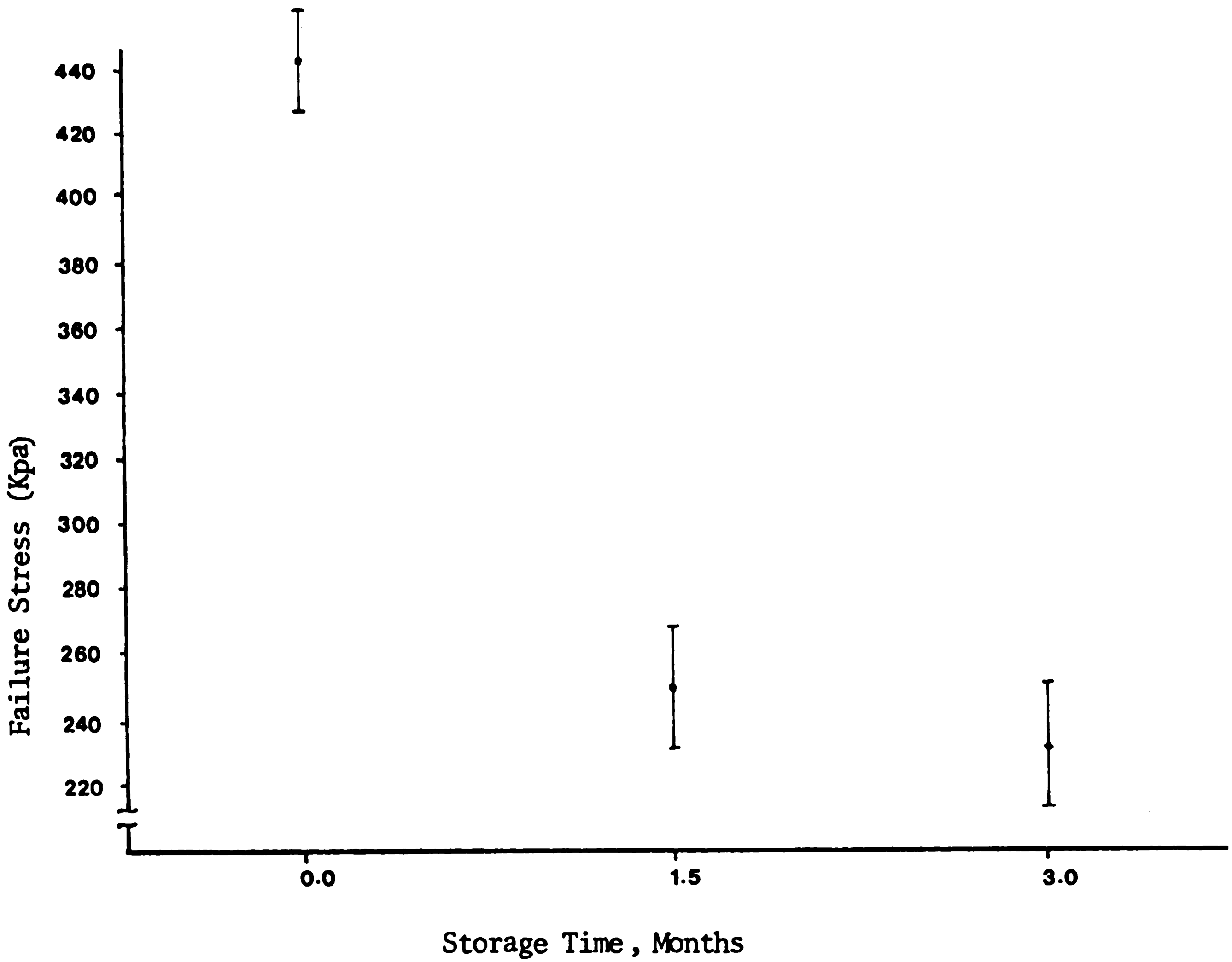

Figure 4.3.-Failure Stress v.s. Storage Time

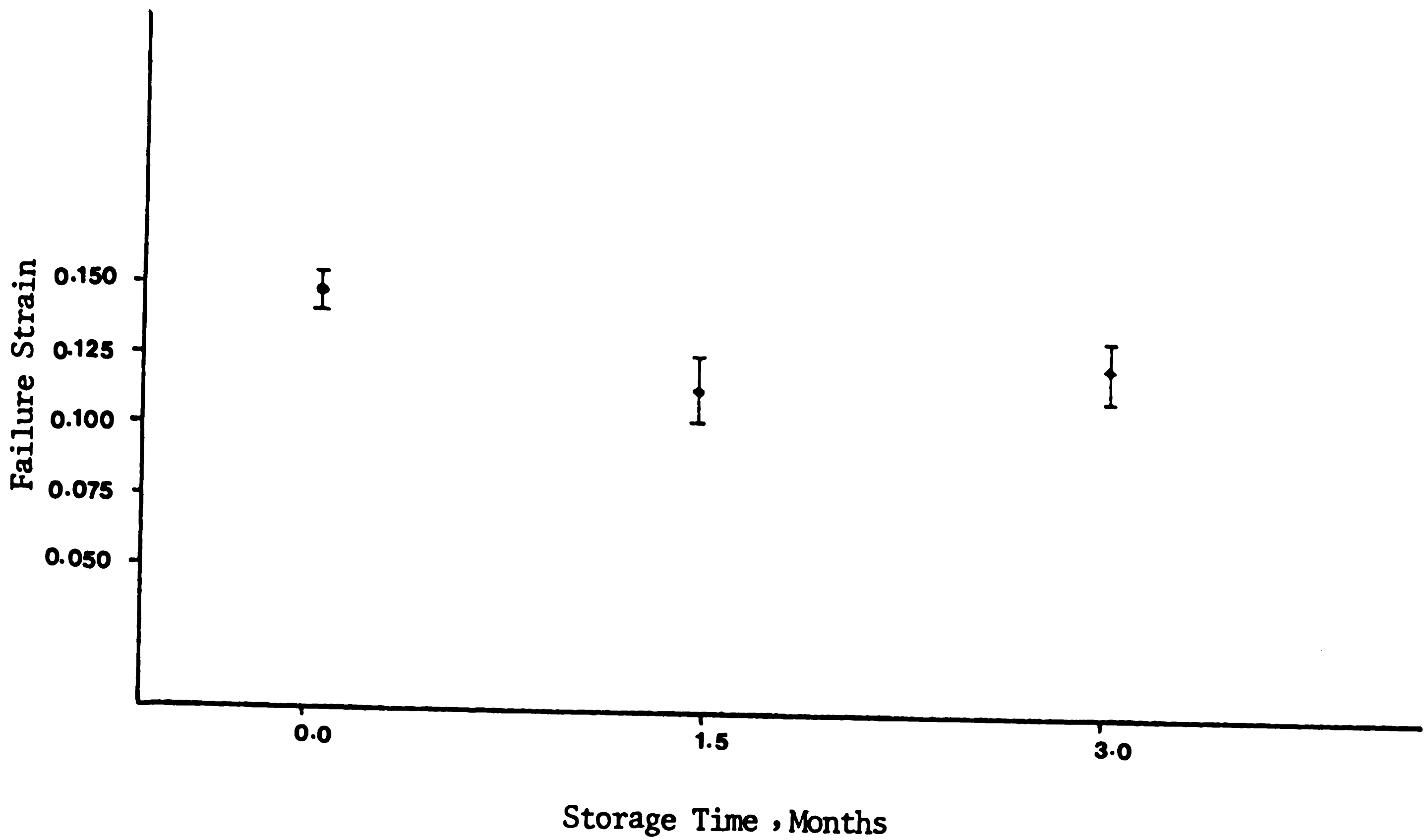

Figure 4.4.--Failure Strain v.s. Storage Time

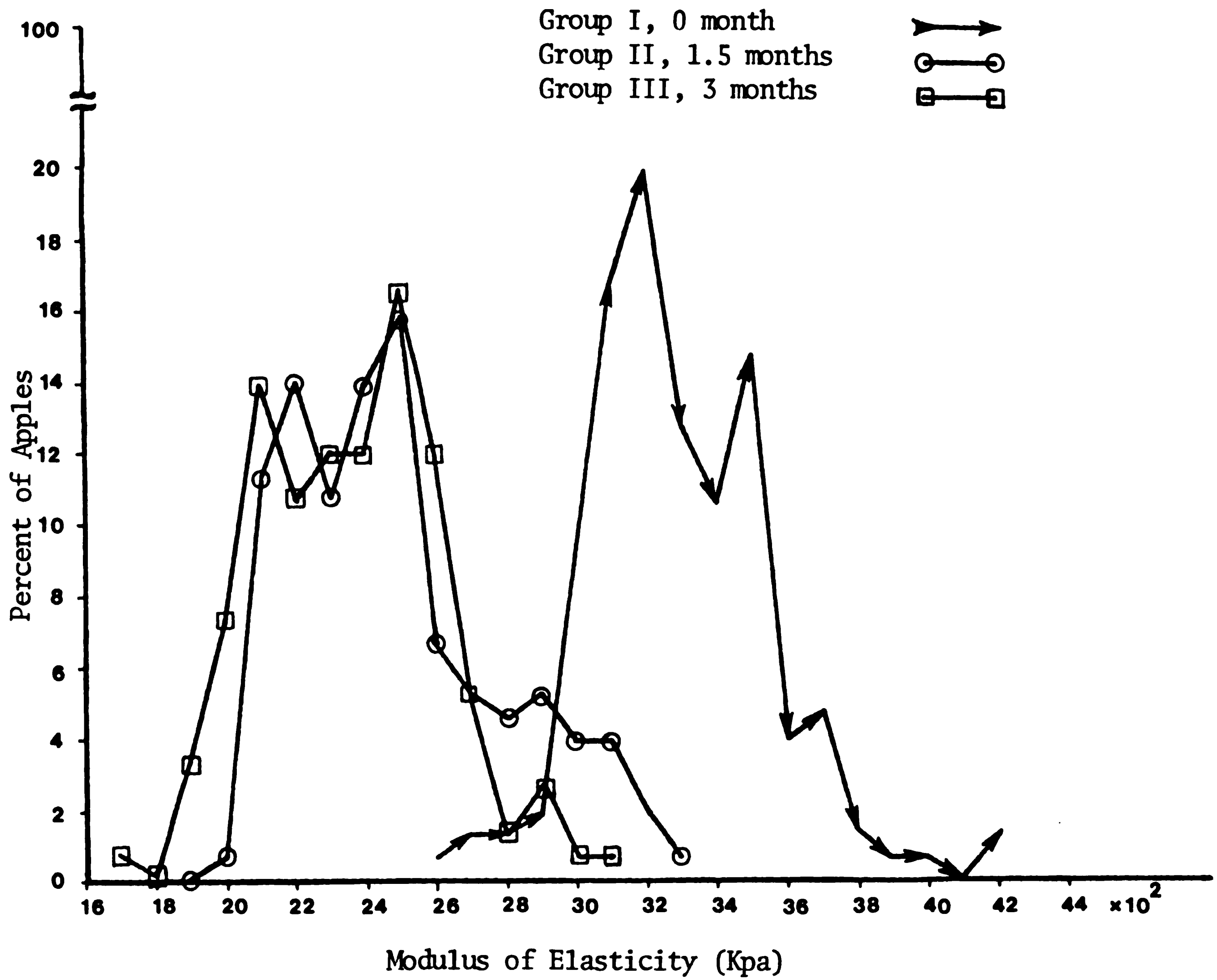

Figure 4.5.--Distribution of the Modulus of Elasticity for 150 Jonathan Apples for the Three Storage Periods.

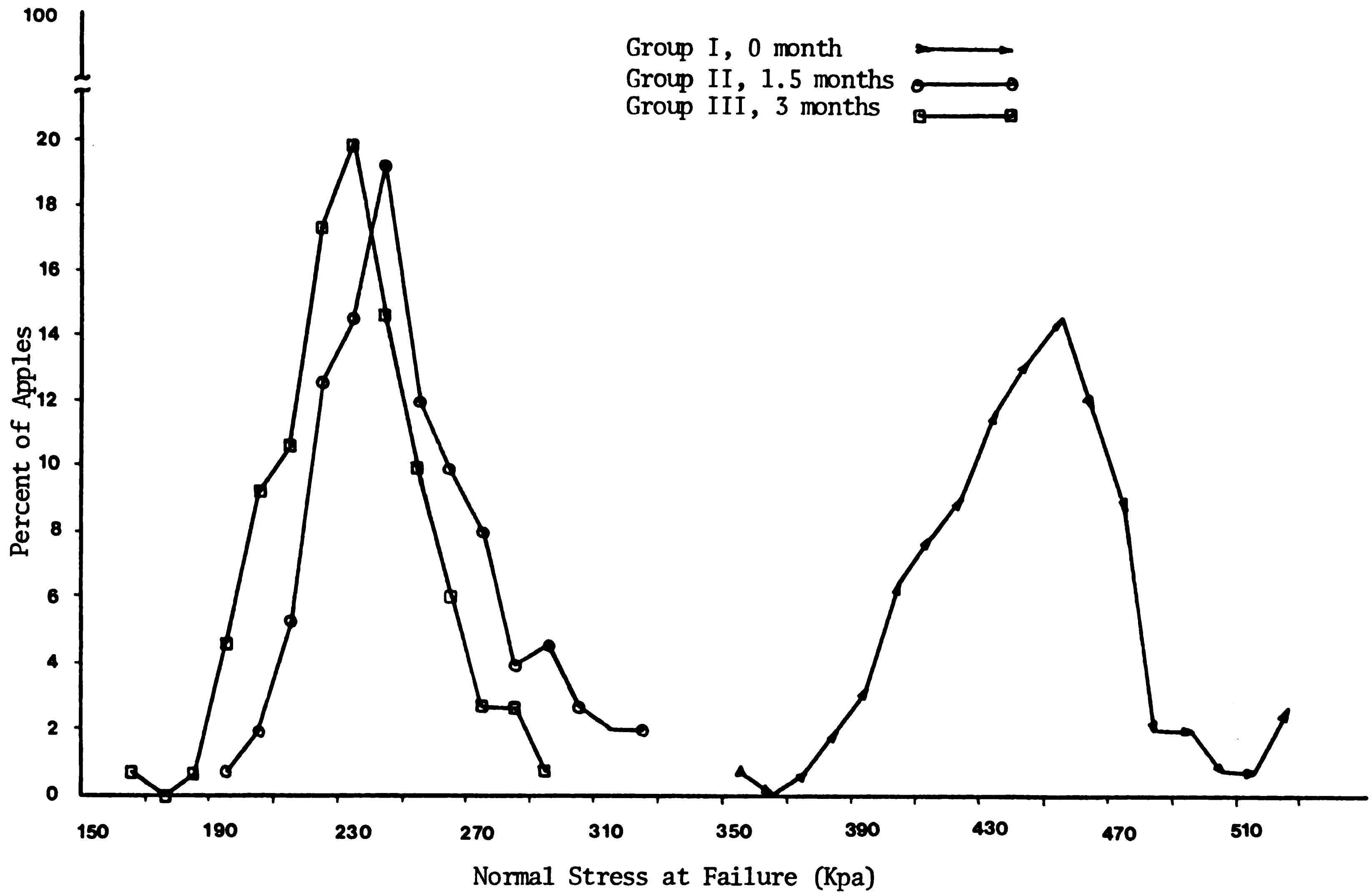

Figure 4.6.--Distribution of Stress at Failure for 150 Jonathan Apples for the Three Storage Periods.

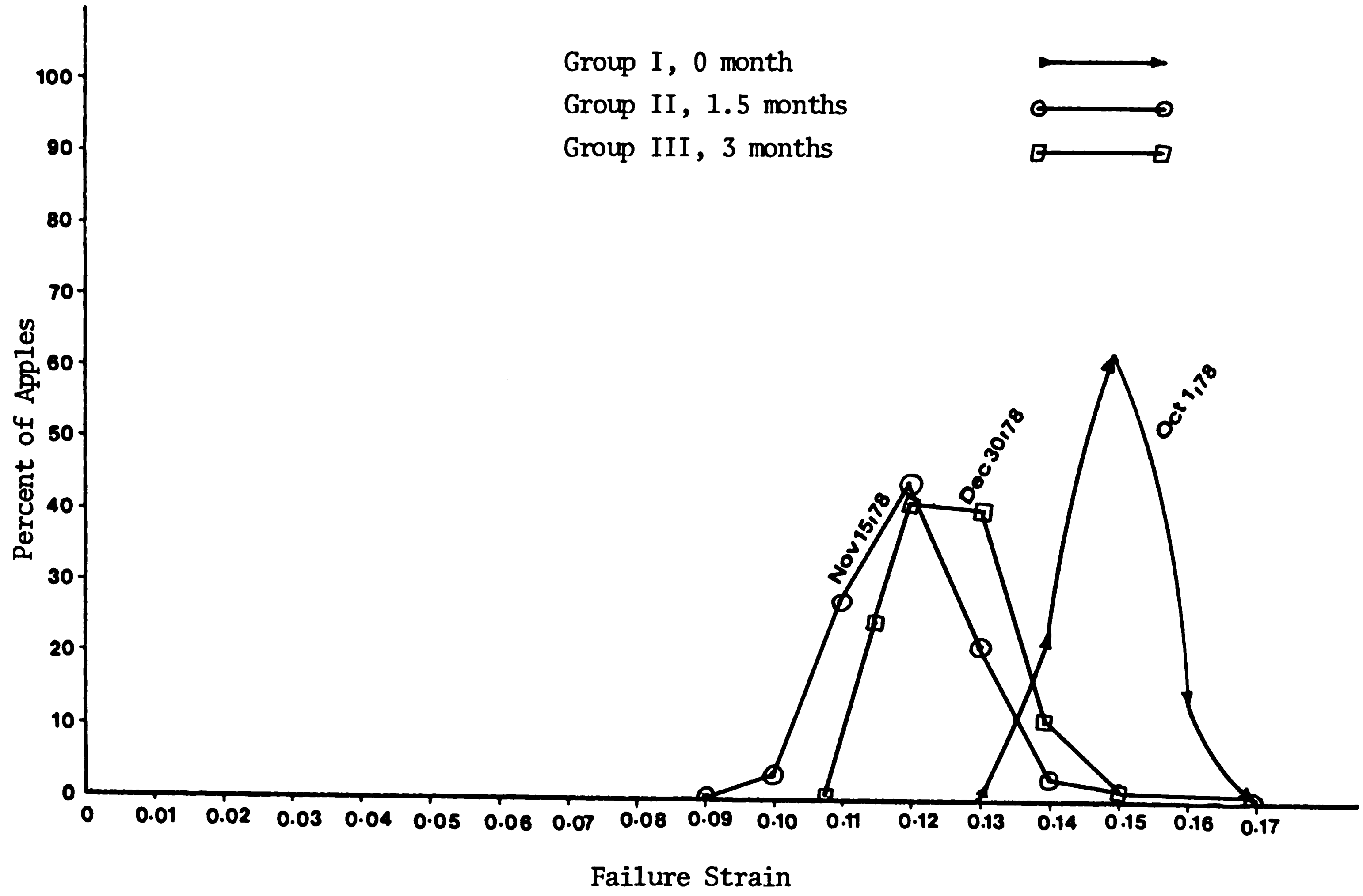

Figure 4.7.--Distribution of Failure Strain for 150 Jonathan Apples for the Three Storage Periods.

V. BRUISE MODEL; ALLOWABLE DEPTH

5.1 Maximum Normal Strain

The bruise model used here to predict the allowable depth for bulk stored apples is based on the failure strain criteria developed by Dal Fabbro (1979). It states that apple flesh fails when a maximum normal strain exceeds a critical value.

The stress components for any point along the z axis were given in Chapter II (2.9). Since failure occurs because of the maximum normal strain, an equation for the maximum normal strain, ε_{zz} is needed. Assuming a homogeneous, isotropic material, Hooke's law gives

$$\varepsilon_{zz} = \frac{1}{E} [\sigma_{zz} - \mu (\sigma_{rr} + \sigma_{\theta\theta})] \tag{5.1}$$

Substituting (2.9) produces

$$\varepsilon_{zz} = \frac{(1 + \mu)q_o}{E} [2\mu[1 - \Psi \operatorname{Tan}^{-1}(\frac{1}{\Psi})] + (1 + \Psi^2)^{-1}] \tag{5.2}$$

The most common contact which occurs in a bulk storage is apple-to-apple contact which can be modeled as the contact between two spheres. To simplify the problem, it was assumed that all apples have the same diameter, 0.0625 m, and a Poisson's ratio of 0.35. The modulus of elasticity and failure strain were treated as random variables.

Using the assumptions on diameter and Poisson's ratio, the radius of contact, (2.7) become

$$a = 0.21745\ F^{1/3} \left[\frac{E_1 + E_2}{E_1\ E_2} \right]^{1/3} \tag{5.3}$$

while
$$q_o = 10.097\ F^{1/3} \left[\frac{E_1 + E_2}{E_1\ E_2} \right]^{-2/3} \tag{5.4}$$

The modulus of elasticity values E_1 and E_2 in (5.3) and (5.4) are for the two apples in contact.

Equation (5.2) gives the maximum strain as a function of Ψ which is equal to Z/a. Given a load F and the modulus of elasticity of each apple, the radius a, (5.3), can be calculated as well as q_o, (5.4). Knowing a and q_o, ε_{zz} can be calculated for any value of z.

Theoretically the location of the maximum value of ε_{zz} can be obtained by differentiating (5.2) with respect to z, setting the resulting equation to zero and solving for z. The resulting equation, however, is not easily solved and it was decided to calculate ε_{zz} for several loadings and moduli values to see how it behaved (see

Appendix D). Examples of some curves for ε_{zz} are shown in Figure 5.1. The average location of the maximum value was 3.65 mm (3.5 - 3.8 mm) for the October 1 data and 3.0 mm (2.8 - 3.2 mm) for the other two sets of data. These values of z were used in the simulation model discussed in the next section because the value of ε_{zz} at 3.65 mm or 3.0 mm differs very little from the maximum value when these values of z are not right at the location of ε_{zz} maximum.

The apples at the bottom of the bin are in contact with a flat hard surface which could be either steel or concrete. In this case E_1 for the steel (or concrete) is much greater than E_2 while R_1 is infinity. These properties modify the equations for a and q_o to

$$a = \left[\frac{F(1715278 + 8.6\ E_2)}{82740000E_2}\right]^{1/3} \tag{5.5}$$

and

$$q_o = 0.4774\ F^{1/3} \left[\frac{1715278 + 8.6\ E_2}{82740000E_2}\right]^{-2/3} \tag{5.6}$$

The location of ε_{zz} maximum for this type of contact was determined in the same manner as for apple-to-apple contact. The location of the maximum values were at z = 3.88 mm (3.55 - 4.21 mm) for the October 1 data and 3.0 mm (2.88 - 3.12 mm) for the other two dates.

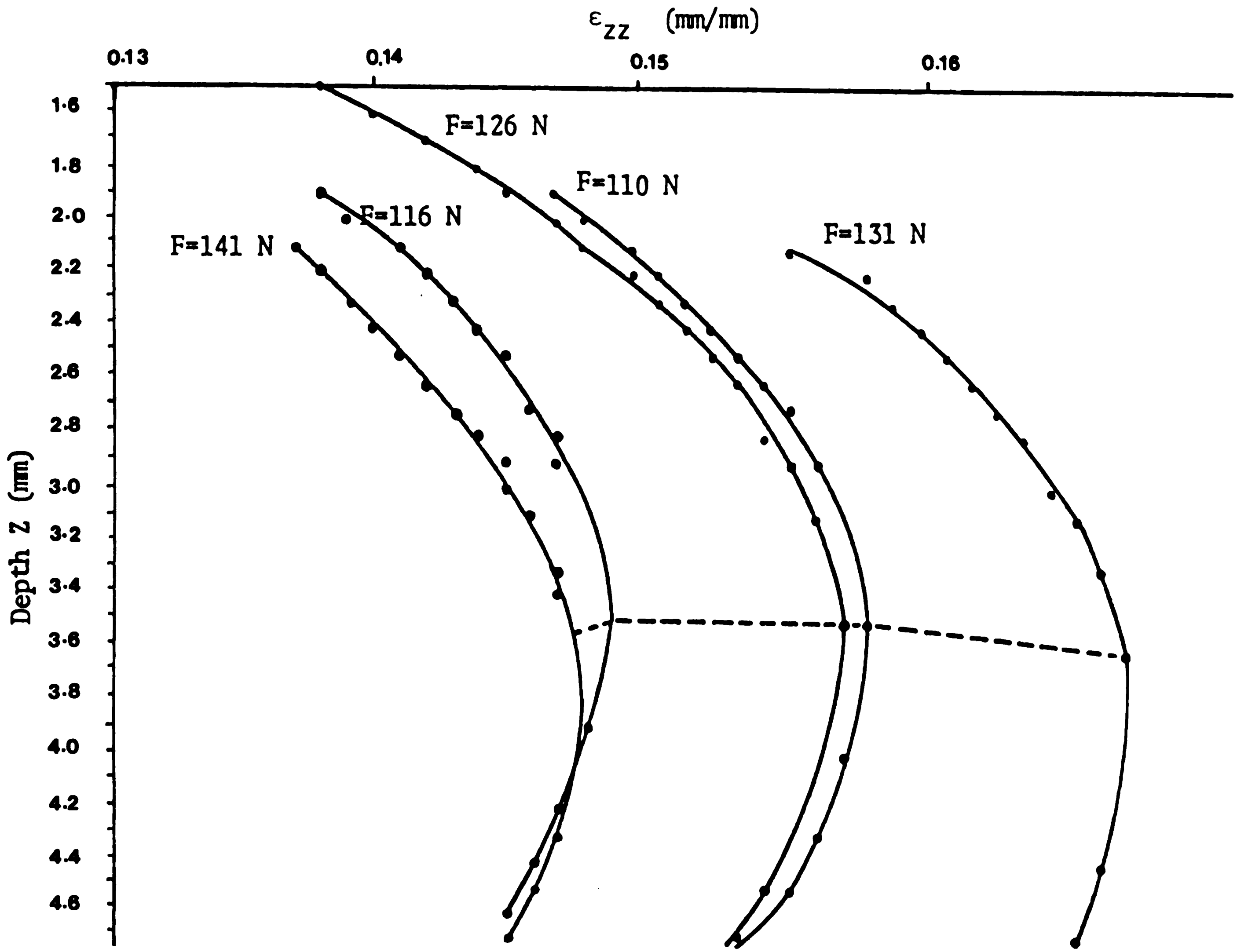

Figure 5.1.--ε_{zz} as Related to Depth. October 1 Data.

5.2 Calculation of the Allowable Storage Depth

The calculation of the allowable storage depth was carried out using (5.2) while treating E_1, E_2 and the failure strain of the pair of apples (or apple in the case of flat plate contact) as a random variable. A normal load F was selected. A random generator was used to select the values of E_1, E_2, ε_{f1}, and ε_{f2} from the data discussed in Chapter IV. The maximum strain in each apple was calculated. If this strain exceeded the failure strain for the apple, the apple was said to be bruised. This calculation was repeated 500 times for each loading. A percent of apples bruised was then calculated. The normal force was increased and the process repeated. The equivalent depth was calculated assuming a single column stack where each apple weighed 0.85 N (Appendix B).

5.3 Results and Discussion

The percent of apples with bruise for each storage group are shown in Figures 5.2 and 5.3. It is immediately obvious that fresh apples can be piled much deeper than apples which have been in storage 1.5 to 3 months. The fresh apples have a significantly larger modulus of elasticity value which means that it takes more force to produce a fixed amount of deformation. There is not an appreciable difference for the results for apple-to-apple

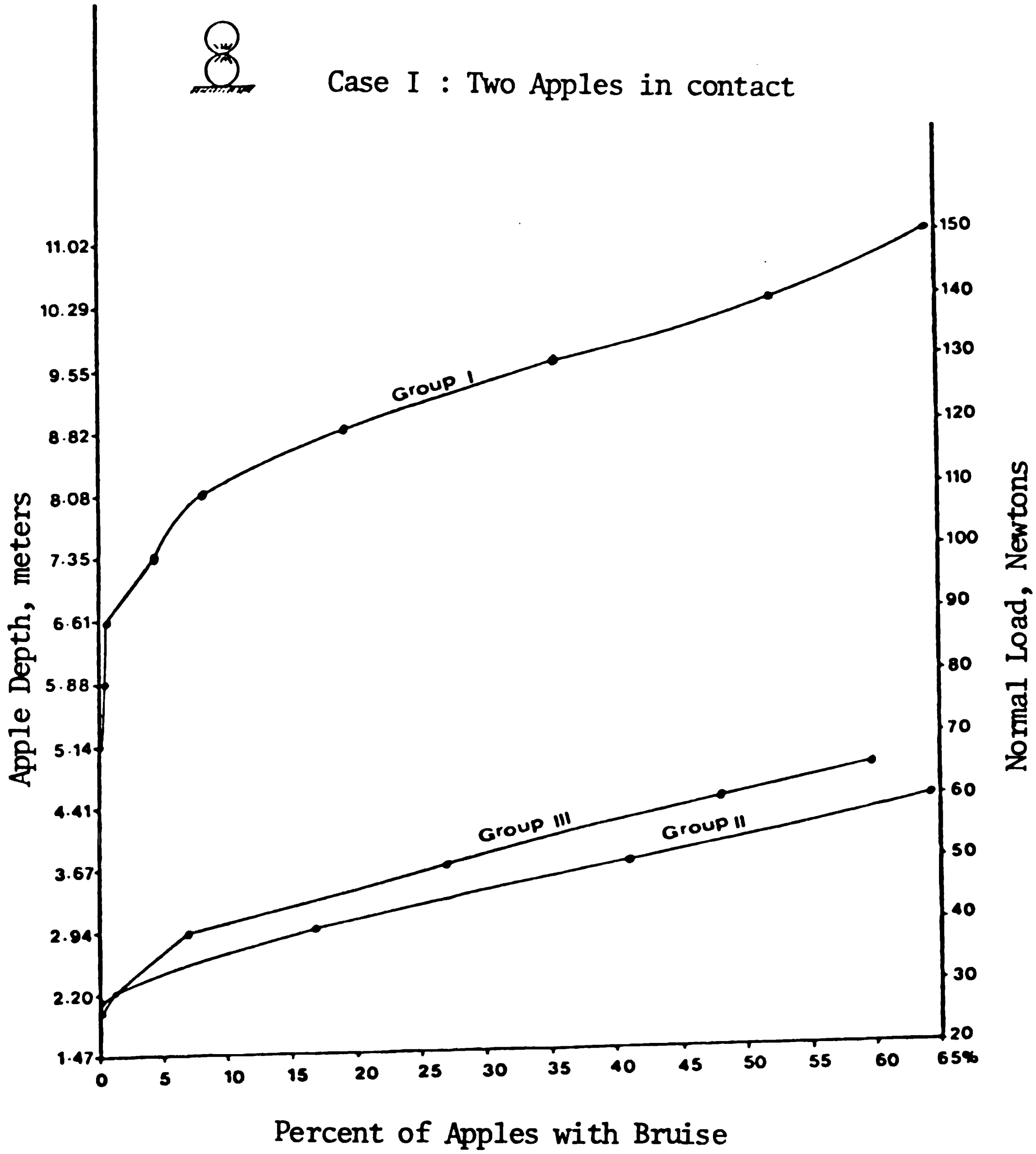

Figure 5.2.--Height and Percent Bruise Relationship for Jonathan Apples in a Bulk Storage (Case I).

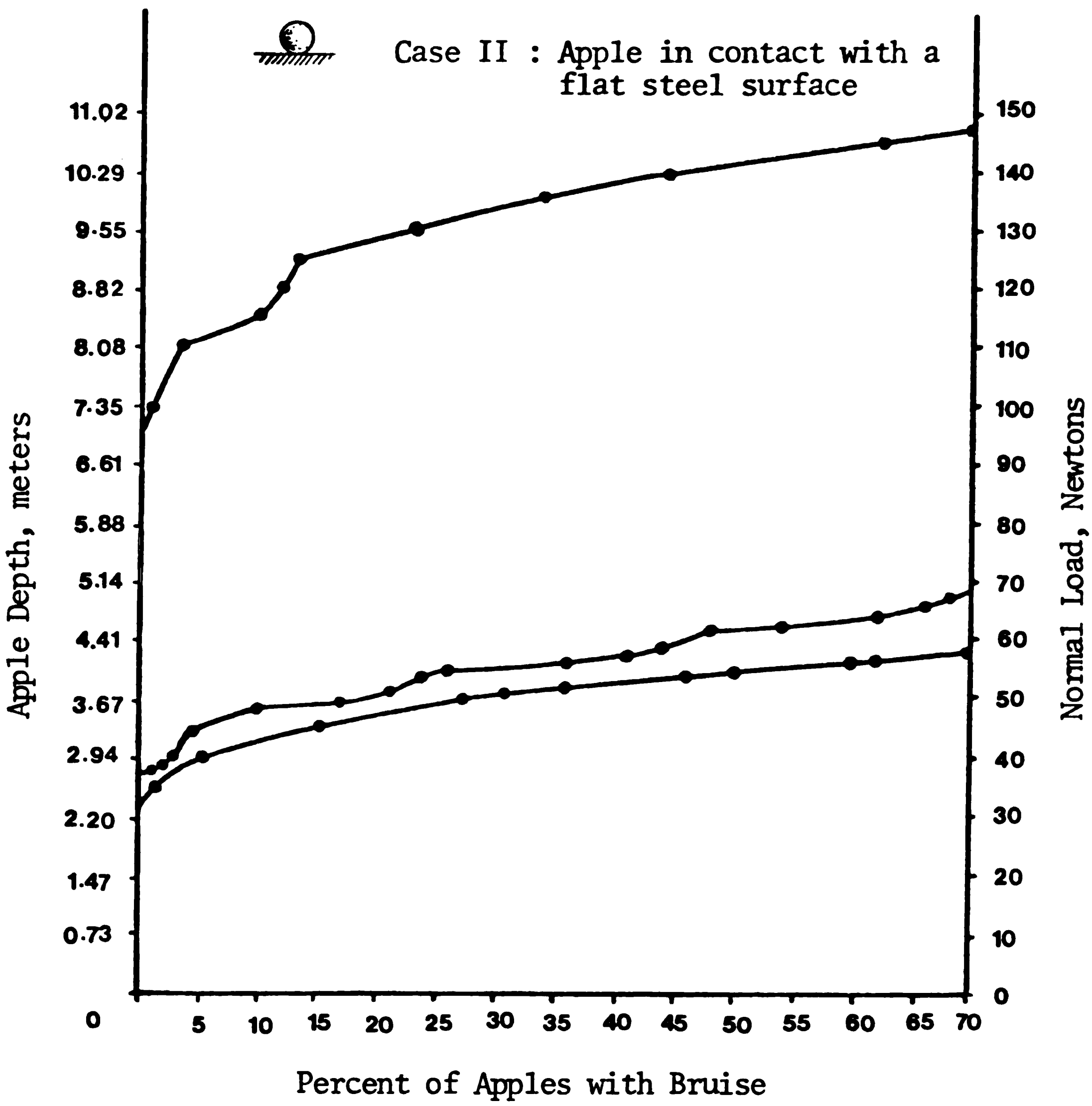

Figure 5.3.--Height and Percent Bruise Relationship for Jonathan Apples in a Bulk Storage (Case II).

contact and the results for apple-to-flat surface contact.

In Figures 5.2 and 5.3 it can be seen that curve for Group III apples is above that of Group II because the value of strain at failure as the failure criterion for Group II was lower than Group III (Figure 4.4).

The curves in Figures 5.2 are used as follows. If an individual wants to store Jonathan apples for three months and is willing to accept 10 percent bruising, these apples can be stored to a depth of about 3 m or 10 feet. This is a conservative estimate, however, because single column contact is not what occurs within a stack and the contact forces on the apple are smaller, allowing a greater depth.

VI. CONTACT FORCE MODEL

6.1 Introduction

The allowable depth for apples stored in bulk that was calculated in the previous chapter assumed a single column stack. This is not what occurs in the actual pile. One apple will contact several others and the actual contact force probably is less. A computer model for calculating the contact force between spherical bodies is presented in this Chapter. An experimental verification using rubber balls is discussed in the next chapter.

The computer model developed here is based on the model developed by Davis (1974). His model is basically a two-dimensional truss analysis where the center of each sphere is considered as the node and the members connecting the nodes have the nonlinear property of two spheres in contact. Davis used small diameter approximately one-half inch diameter, steel balls in his study. Six centimeter diameter rubber balls were used in this study. The sphere is much larger and softer.

The following simplifications were made.

a. The spheres are assumed to be identical and only two-dimensional packing problem is considered, i.e., each sphere in the assemblage of spheres has its center on a common plane.

b. Only normal forces at the sphere contacts are considered (shear forces are neglected due to small magnitudes) and the Hertz theory is used to relate the magnitudes of such forces to the corresponding sphere compression.

c. Arrangement of spheres in a sample is assumed to be in a geometrically stable configuration. The initial configuration for this analysis, therefore, must be taken so that no gross movement or rearrangement of the spheres will occur during uniform pressure loading.

e. The change in the contact area is due to the small compressions at the sphere contacts rather than the gross change in the packing geometry.

6.2 Model Formulation

Considering a small stable sample of identical spheres arranged in two-dimensional rhombohedral system and loaded at the top by a uniform pressure, Figure 6.1. The information in Figure 6.1 is shown in Figure 6.2 in the form of a planar graph which is obtained by connecting the center of the spheres. The nodes of the graph in

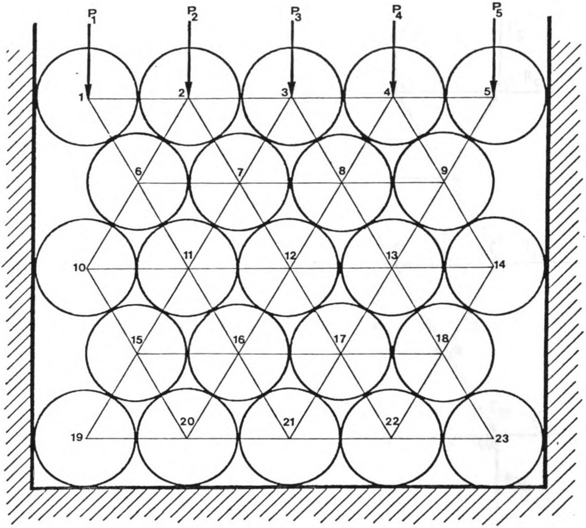

Figure 6.1.--Two Dimensional Rhombohedral Packing of Identical Spheres Subjected to Uniform Pressure Loading at the Top

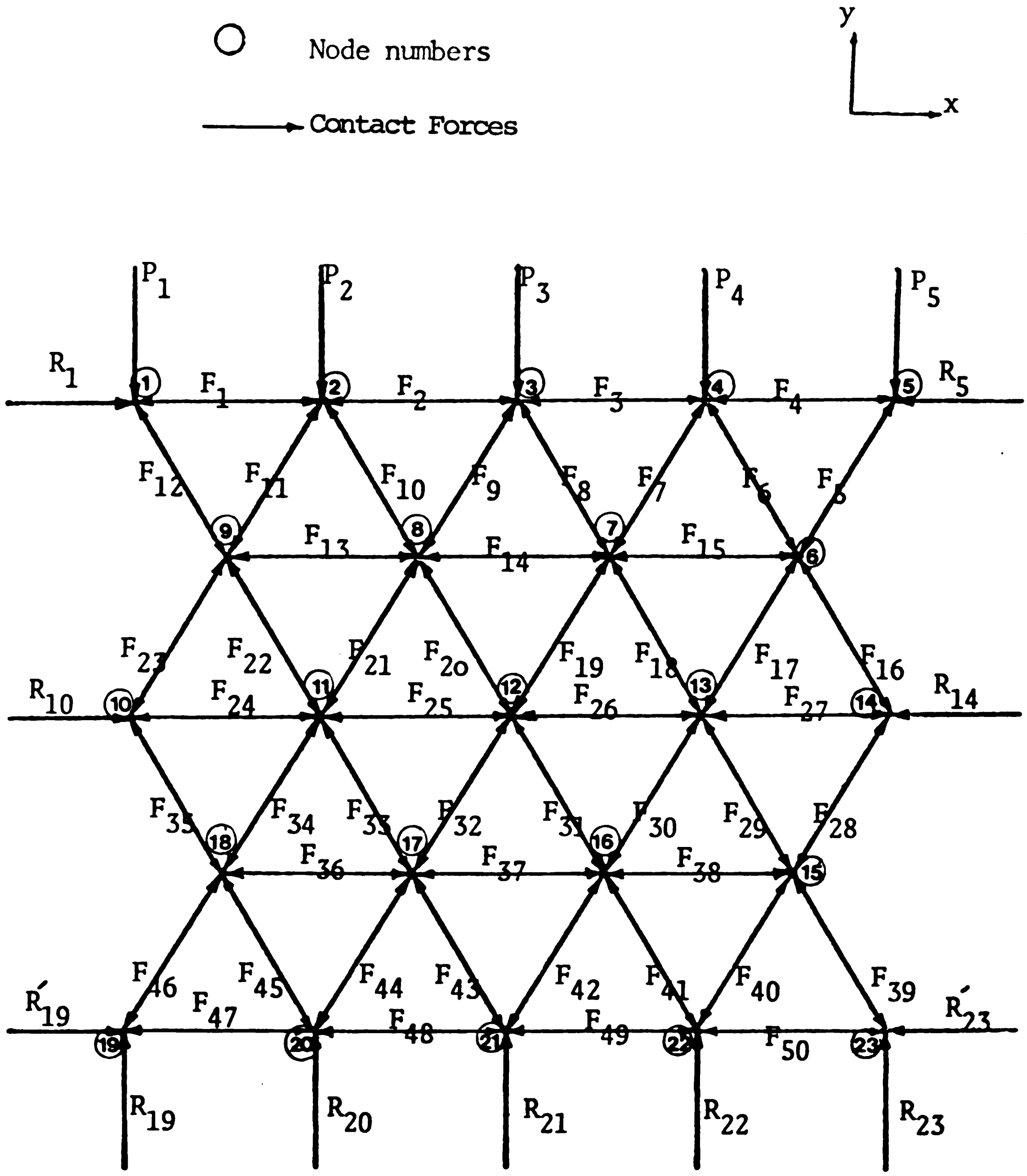

Figure 6.2.--Planar Graph Representation of Figure 6.1 and Corresponding Contact Forces.

Figure 6.2 represent the sphere center and branches of the graph correspond to the contacts between adjacent spheres. Since shear components of the contact forces are neglected, forces are transmitted throughout the packing along the branches of the planar graph. The task is to find the forces at each of these branches and study their distribution in the bin where they are located. As mentioned before, since the initial configuration of the assemblage is geometrically stable and no sphere will be moved or dislocated, only a small compression at the contact points of the spheres will occur during the loading. In structural analysis, members (branches) are idealized as lines which meet at points (nodes) which are called joints, so the problem formulation can be employed and the displacement of the sphere centers are introduced as unknowns.

Assuming that the rigid-body degrees for the assemblage have been removed by the introduction of appropriate supports, the equilibrium equations for each movable joint of the assemblage may be written as:

$$[N]\,\{F\} = \{P\} \qquad (6.1)$$

where $\{F\}$ is the $(B \times 1)$ matrix of contact force magnitude and it is customary to assume the contact forces positive when they are in compression (B is the number of bars).

{P} represents (2J x 1) matrix of applied node forces where J is the number of joints or nodes.

[N] is a generalized branch node incidence matrix or simply an incidence matrix.

To understand the construction of [N] consider Figure 6.3.

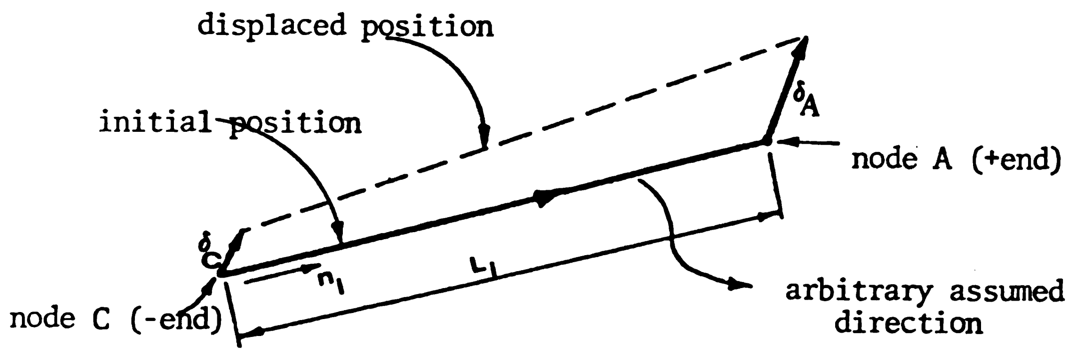

Figure 6.3.--Representation of Member i.

Figure 6.3 shows a typical truss bar and the associated with which is the bar force F_i and the bar length change Δ_i, chosen so that positive F_i and Δ_i corresponds to tension or stretching within the bar and a unit vector n_i. Knowing the displacement of the ends of a bar, it is possible to compute the change in length of the bar by the following relationship

$$\Delta_i = n_i \ (\delta_A - \delta_c) \tag{6.2}$$

which involves projecting the joint displacement vector along the original position of the bar. Equation 6.2 can be written for the entire structure as

$$[\Delta] = [N]\ \{\delta\} \tag{6.3}$$

where [N] is a (B x J) = (row x column) matrix whose elements N_{ij} are

$$N_{ij} = \begin{cases} n_i \text{ if node } j \text{ is the positive end of branch } i \\ -n_i \text{ if node } j \text{ is the negative end of branch } i \\ 0 \text{ otherwise} \end{cases}$$

B and J are the number of bars and joints, respectively. $\{\delta\}$ is the node displacement matrix.

In the circular assemblage of Figure 6.1, B is the number of contact points and J is the number of movable nodes. From elementary mechanics of solids it is known that the bar forces and displacement are related through Hooke's law, in which

$$F_i = K_i\ \Delta_i \tag{6.4}$$

The Hertz contact theory applied to the ith contact yields (Davis, 1974):

$$F_i = \begin{cases} k \quad \Delta_i^{3/2} & , \quad \Delta_i \geq 0 \\ 0 & \quad \Delta_i < 0 \end{cases} \tag{6.5}$$

where $K = 2G \sqrt{2R} /3 (1-\mu)$

k is a constant which depends on the radius and elastic properties of spheres

G and μ are shear modulus and Poison's ratio, respectively.

Equations (6.1), (6.3) and (6.5) can be combined in the usual manner for the node formulation and written (Zienkiewicz, 1971)

$$[N]^T[K(\delta)][N]\{\delta\} = \{P\} \tag{6.6}$$

where [N] is (B x B) transformation matrix

$[K(\delta)]$ is the (B x B) diagonal Hooke's law matrix

$\{\delta\}$ is (2J x 1) deflection vector

$\{P\}$ is (2J x 1) external load vector

Equation (6.6) represents a set of 2J simultaneous, non-linear equation for the unknowns $\{\delta\}$.

6.3 Calculations

The objective here is to use the formulation of the previous section to calculate the joint deflections and then the forces between the uniform spheres arranged in the two-dimensional rhombohedral system shown in Figure 6.1.

The displacements for all nodes are not the same. Nodes 1, 5, 10 and 14 can move only in the y-direction while nodes 19, 20, 21, 22 and 23 cannot move in either direction. Each of the rest of the nodes can move in both the x and y directions.

Using the appropriate degrees of freedom for each node, there are 32 force equilibrium equations. Since there are 50 contact forces between spheres, the transformation matrix has a dimension of (32 x 50) and can easily be constructed from the force equilibrium equations. The transformation matrix is in fact the direction cosines of the branches in the assemblage which for rhombohedral system would be either cos 60° or cos 30° depending on the location of the nodes and branches.

It is necessary to have values for k and Δ_i to calculate F_i in (6.5). A value for Δ_i is necessary because (6.5) is nonlinear in Δ_i. An arbitrary value of -0.254 cm was assumed for each component of $\{\delta\}$. Equation (6.3) was then used to calculate each Δ_i. Assuming Cos 30° for each component of transformation matrix in first iteration, the value of Δ_i will be 0.254 cm.

To determine the value of k in (6.5) a single rubber ball, 6.09 cm diameter, was marked with a small drop of black ink. A sheet of white paper was placed between the ink spot and the rigid flat circular head of the Instron machine. After exerting a load of 72 Newtons the radius of the contact area of the ball on the white paper was measured to be a = 1.2 cm.

Timoshenko gives the radius of contact area as

$$a = \sqrt[3]{\frac{3\pi F(K_1 + K_2)\ R_1R_2}{4\ (R_1 + R_2)}} \qquad (6.7)$$

where $K_1 = \frac{1-\mu_1^2}{\pi E_1}$ and $K_2 = \frac{1-\mu_2^2}{\pi E_2}$

F is the applied load

R_1 and R_2 are the radius of the two spheres in contact.

E and μ are modulus of elasticity and Poisson's ratio.

Assuming the rigid plate of the base of Instron has $E = \infty$ when compared with rubber ball and its radius is equal to infinity, (6.7) reduces to

$$a = \sqrt[3]{\frac{3\pi FK_1R_1}{4}} \qquad (6.8)$$

Substituting the appropriate values in (6.8) K_1 would be

$K_1 = 0.003345\ cm^2/N$

To find the value for μ_1, a cubical specimen of one centimeter in dimension was carefully cut from the rubber ball, and was loaded in the Instron machine and the strain perpendicular to the load and parallel to the load were measured. Poisson's ratio was determined to be μ = 0.13.

Using $\mu = 0.13$ and $K_1 = 0.003345$, E_1 was calculated as $E_1 = 93.55\ \mathrm{N/cm^2}$ and the shear modules becomes

$$G = \frac{E}{2(1+\mu)} = 41.39\ \mathrm{N/cm^2}$$

Since $\quad k = 2G\sqrt{2R}\ /\ [3(1-\mu)]$

Substitution gives $k = 78.26\ \mathrm{N/cm^{3/2}}$

The diagnonal terms of $[K(\delta)]$ in (6.6) are each given by

$$k_{ii} = k\ (\Delta_i^{1/2})$$

or $\quad k_{ii} = -39.44\ \mathrm{N/Cm}$

Since (6.6) is a nonlinear equation, it must be solved using iterations until the calculated displacements on two successive iterations differ by less than a specified amount. Convergence to the solution was obtained in about 18 iterations for the problems discussed in the last section (see Appendix C).

6.4 Results

Table 6.1 gives the values of the nodal deflections for the configuration of Figure 6.2 with a concentrated load of 45 N applied at each of the upper nodes. These values are also shown in Figure 6.4. The contact forces are shown in Figure 6.5. The contact forces for other loading situations are given in Figures 6.6, 6.7, and 6.8.

Table 6.1. Deflection of nodes in x and y direction of a two dimensional rhombohedral assemblage for 45 N of load at each node (18 iterations)

Node No.	Deflection in X direction (mm)	Deflection in Y direction (mm)	Node No.	Deflection in X direction (mm)	Deflection in Y direction (mm)
1	0	-31.82	13	-1.34	-13.61
2	-0.304	-25.04	14	0	-13.10
3	0	-23.90	15	-0.15	- 6.47
4	0.304	-25.04	16	-0.43	- 6.78
5	0	-31.82	17	-0.43	- 6.80
6	-2.64	-21.18	18	0.15	- 6.47
7	-0.68	-18.56	19	0	0
8	0.68	-18.56	20	0	0
9	2.64	-21.18	21	0	0
10	0	-13.10	22	0	0
11	1.34	-13.61	23	0	0
12	0	12.77			

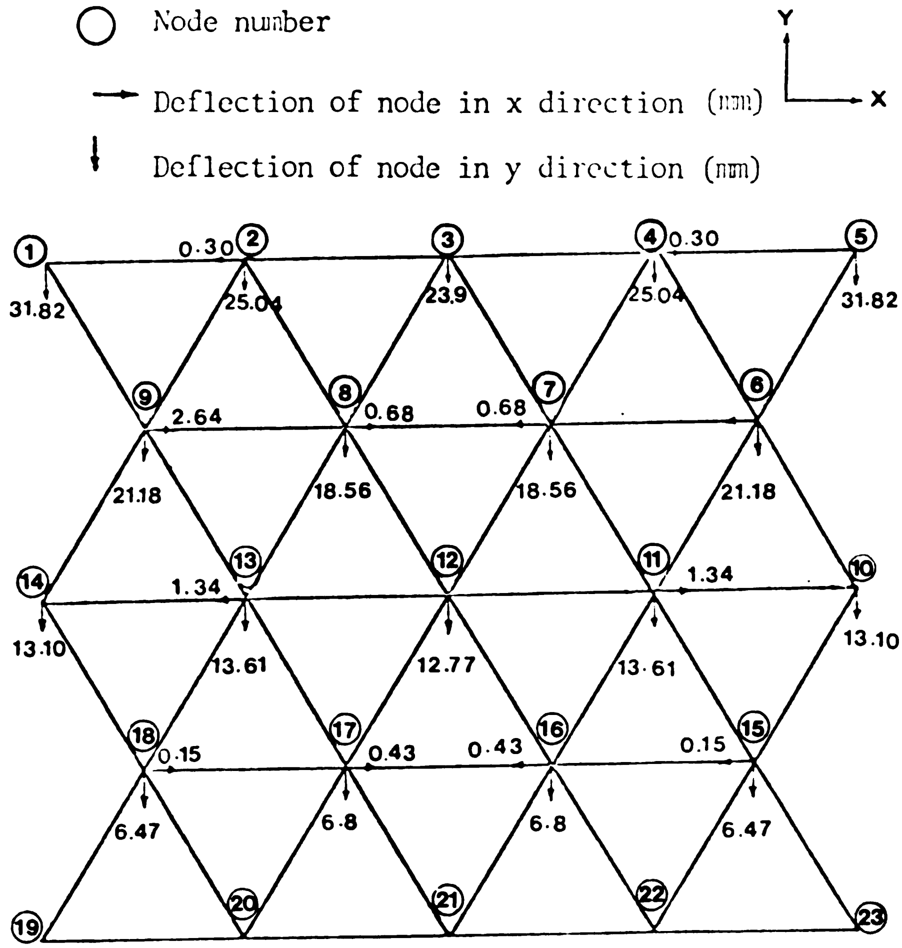

Figure 6.4.-- Planar Graph Representation of Deflection of Nodes in x and y direction when 225 N Load was exerted

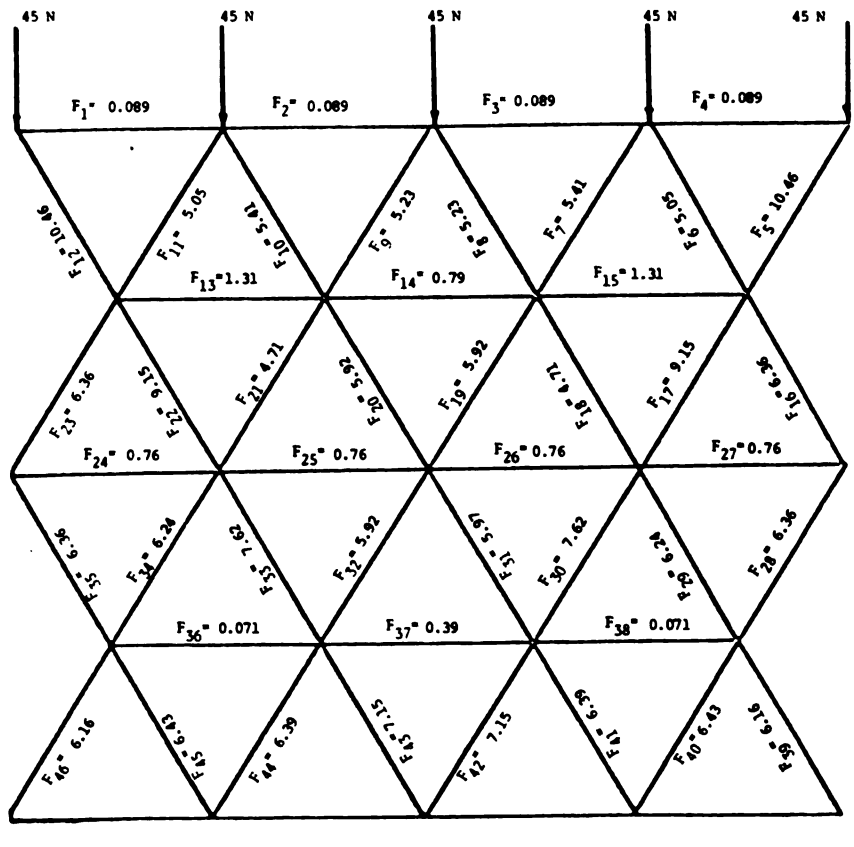

Figure 6.5.--Planar Graph Representation of Calculated Contact Forces for a 225 N Load. All Values in Newtons.

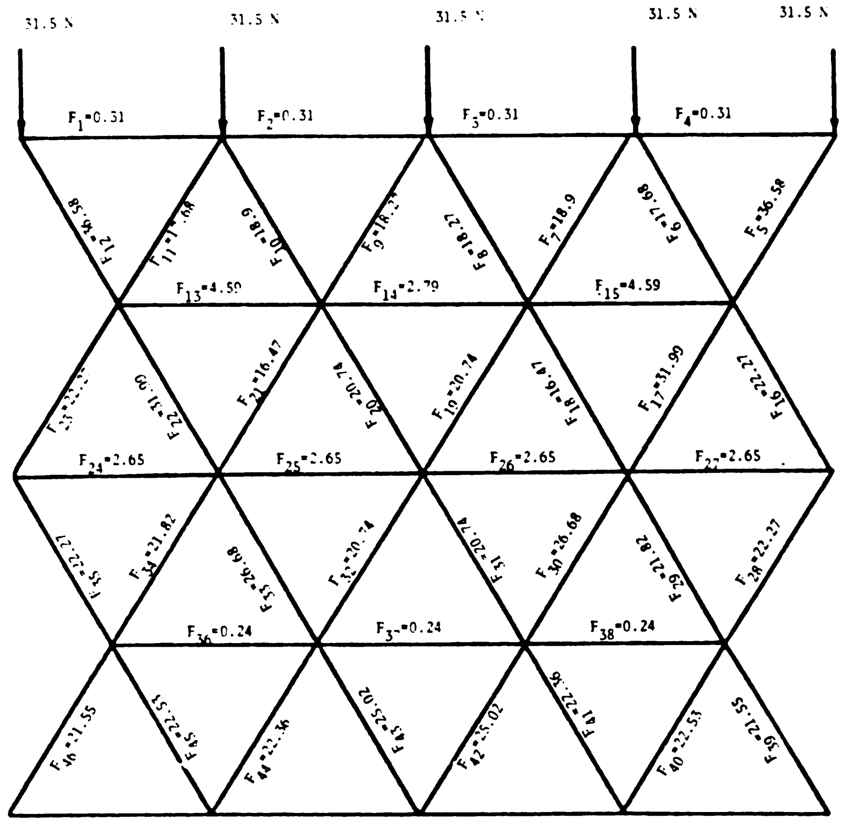

Figure 6.6.--Planar Graph Representation of Calculated Contact Forces for a 157.5 N Load. All Values in Newtons.

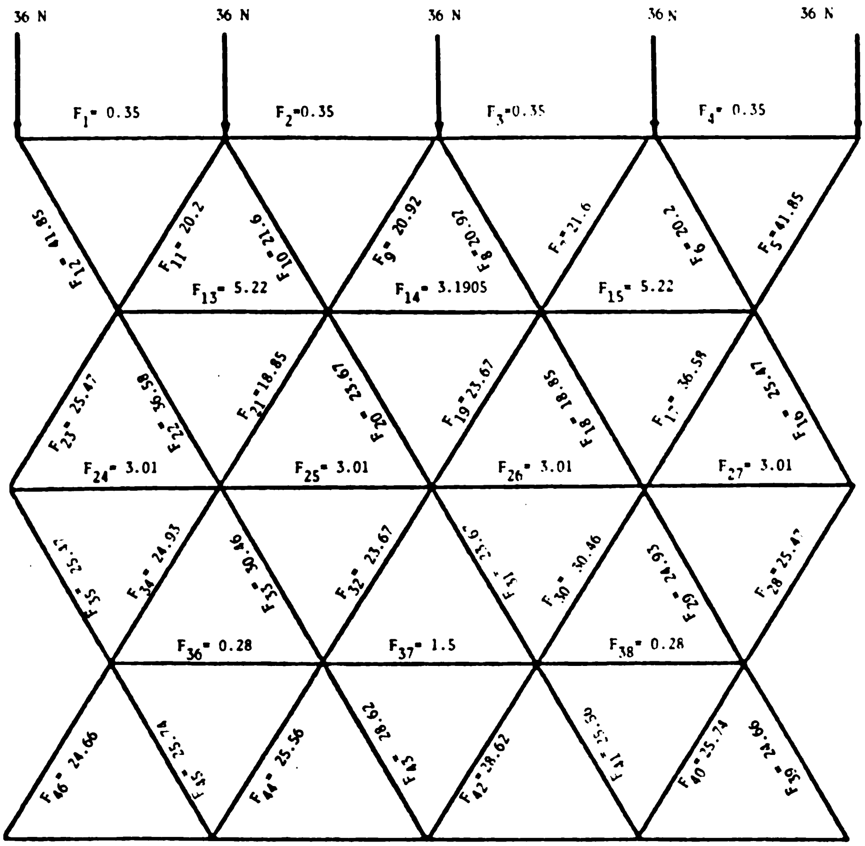

Figure 6.7.-- Planar Graph Representation of Calculated Contact Forces for a 180 N Load.
All values in Newtons

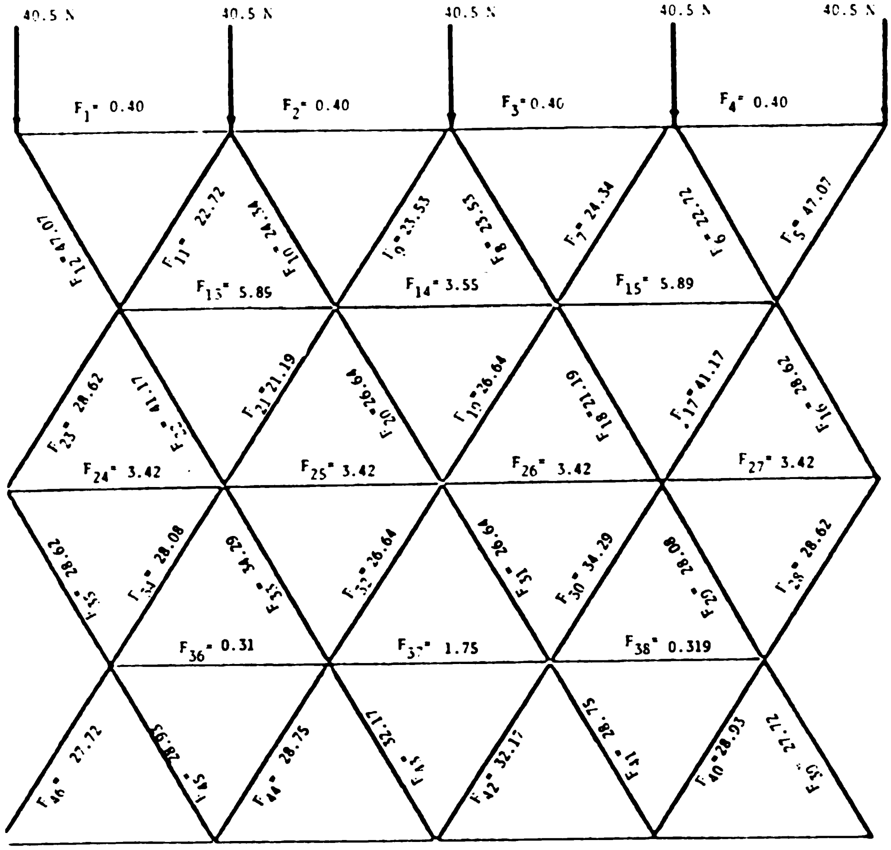

Figure 6.8.--Planar Graph Representation of Calculated Contact Forces for a 202.5 N Load. All the Values in Newtons.

VII. EXPERIMENTAL INVESTIGATION OF THE CONTACT MODEL

7.1 General Remarks

To simulate the force distribution between bodies in contact in a bulk storage of apples, a series of tests were conducted in the laboratory. In order to have some uniformity in the granular material, it was decided to use rubber balls with an average diameter of 6.25 to 6.85 cm which is close to that of Jonathan apples. A simple case of two dimensional packing with a rhombohedral assemblage was used. The total of twenty-three balls was used with five balls in a row and five rows in a rhombic manner.

In order to insure that the rubber balls were similar in size and stiffness, the balls were sorted by diameter and then by stiffness. The stiffness was measured using a flat plate test on the Instron Testing machine. The stiffness criteria was that the balls should require between 54-63 N to produce a 1.7 cm deflection. Several portions on each ball were tested.

7.2 Equipment

1. Test Box: A wooden box 53 cm high, 32 cm wide and 6.8 cm thick was constructed. The box was made

with these dimensions so that it could be loaded using an Instron testing machine and could hold five rubber balls in each layer with a little gap for the installation of the pressure transducers. The perforated plexiglass window of the box was easily assembled or removed so that the connecting wires from the pressure transducers could extend from the box to the strain indicator, Figure 7.1.

2. Loading Piston: To exert the load in a uniform manner from the head of the Instron to the balls in the testing box, a loading pistion was constructed, Figure 7.2.

The piston consisted of a metal strip to which the supporting bars were connected. A wooden layer (1.5 cm thick) and a foam layer (2.5 cm thick) were attached on the bottom side of the metal strip. The piston had rectangular cross-section with dimension of (31.5 cm x 6.5 cm) which would fit into the top of the testing box.

3. Pressure Transducer: A special pressure transducer was designed for the experiment and is shown in Figure 7.3. The pressure transducer consisted of a 3.2 x 2 cm upper plate 0.5 mm thick. It was made from spring steel. A lower plate, with the same dimensions except it was thicker (1 mm), was made from hard steel. Two millimeter diameter rollers, two cm long, were glued to the bottom plate. The upper plate rested on the

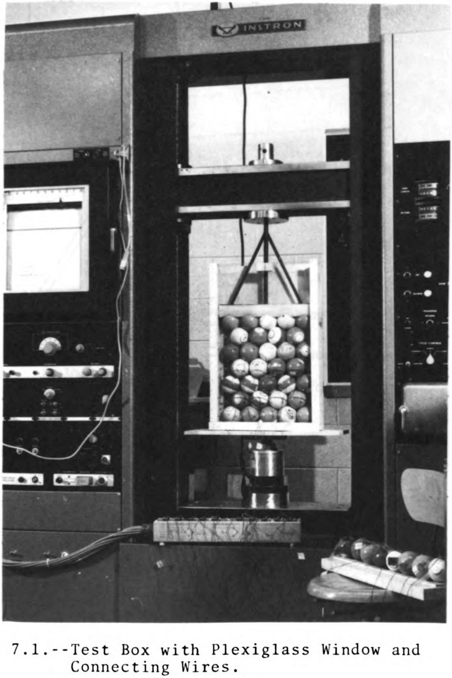

Figure 7.1.--Test Box with Plexiglass Window and Connecting Wires.

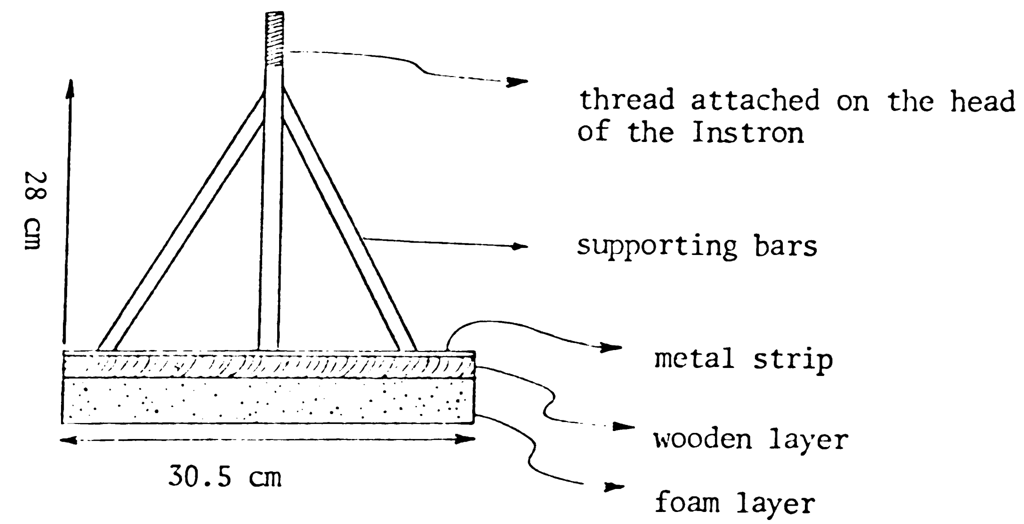

Figure 7.2.--Different Parts of Loading Piston.

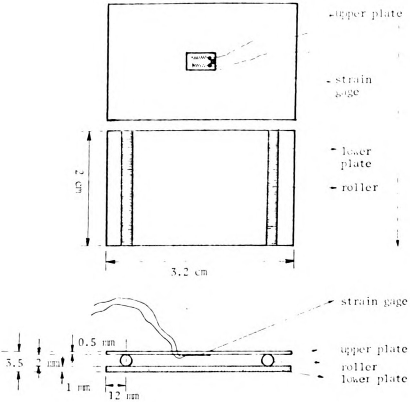

Figure 7.3.--Dimensions and Assemblage of the Pressure Transducers.

rollers. A strain gage, (Micro Measurement EA-06-250BG-120) was attached to the lower surface of the upper plate. The upper plate acts as a simply supported beam and was used to determine the magnitude of a load once it was calibrated.

4. Multi-Channel Digital Strain Indicator 161-mini-system: The strain gage transducer was attached to a model 161 (B & F Instrument, Inc.) digital strain indicator. This apparatus had ten channels and a terminal box where the pressure transducers and their compensating gages were connected, Figure 7.4 and 7.5.

5. A model OD-1014 printer was connected to the multi-channel Digital strain indicator. Total of twenty pressure transducers were made, of which eight were used compensating gages.

7.3 Calibration of Gages of Pressure Transducers

Each pressure transducer was assembled and connected in a singel active arm bridge form to the strain indicator and calibrated. Calibration was done by gluing one of the rubber balls on the head of the Instron machine and locating the transducer beneath the ball on the load cell of the Instron, Figure 7.6. Different levels of load were exerted on the transducer and the corresponding strain was read from the strain indicator and a

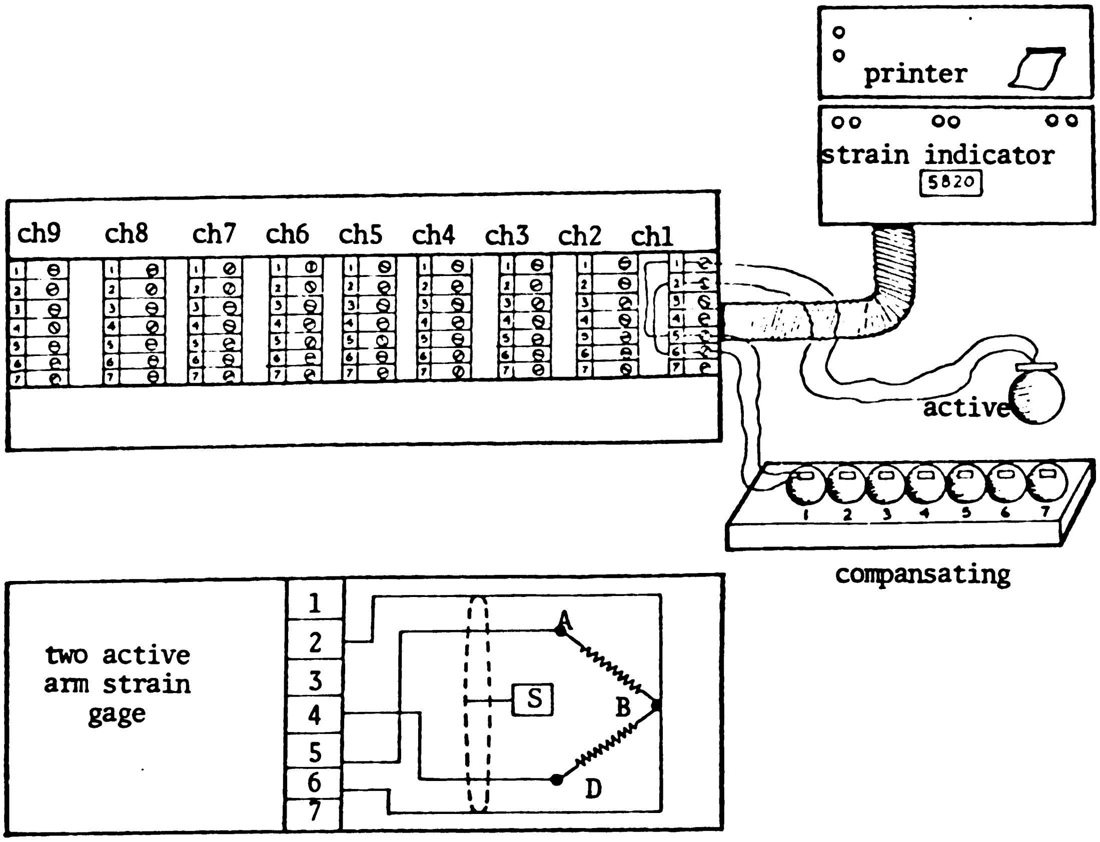

Figure 7.4.--Terminal Box of Multichannel Digital Strain Indicator.

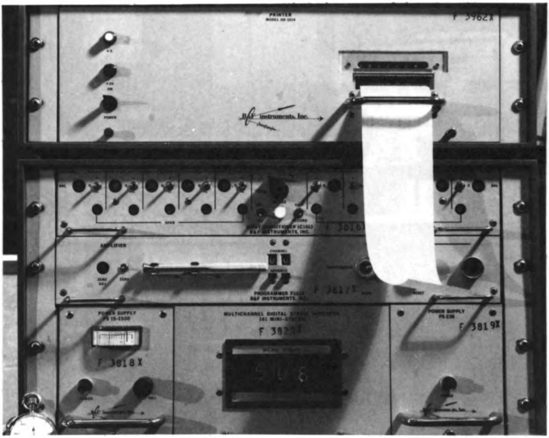

Figure 7.5. Multi-Channel Digital Strain Indicator with Model OD-1014 Printer

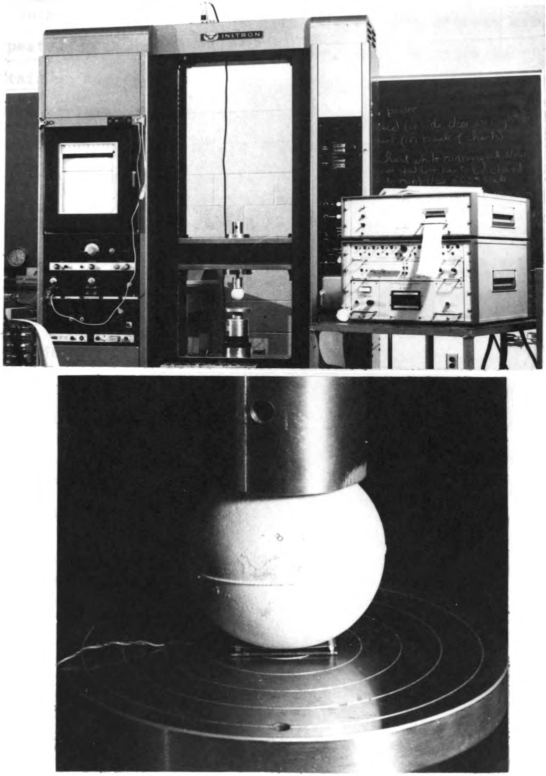

Figure 7.6. Calibration of Pressure Transducer

calibration curve for each gage was obtained. An example of such a curve is given in Figure 7.7. This process was repeated at least five times for each gage in order to obtain an average curve. The average calibration curve had a variation of ± 3% from the other curves at a maxi= mum load of 90 N (20 lbs.). Example force and corresponding strain data are given in Table 7.1.

7.4 Experimental Procedure

First step was to connect the eight pressure transducers and the eight corresponding compensating gages to the digital strain indicator. Digital strain indicator was adjusted for R_{cal} = 1474 Ω from the table of calibration set points based on 120 Ω single active arms input and gage factor of 2.03. Since there was just one active gage in the pressure transducer, a compensating gage was placed on the steel plate, outside the text box and a two arm-bridge hook-up was used.

7.4.1 Pressure Transducer Placement

The objective was to measure the contact forces at as many contact points in the assemblage as reasonably possible. The eight pressure transducers allowed the contact force at eight different points to be measured at a time. The attachment of the transducers on the exact contact points in the assemblage was very important.

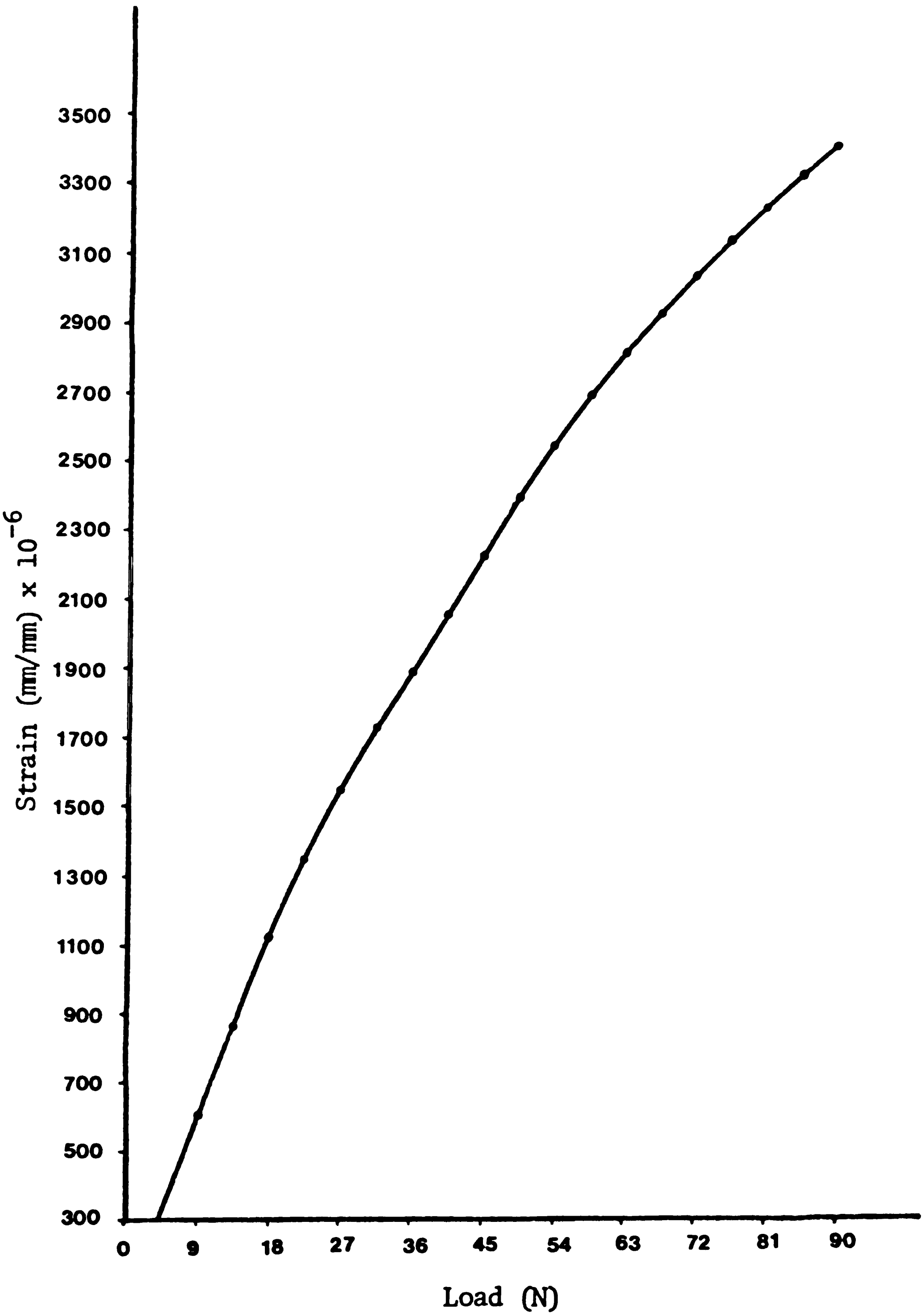

Figure 7.7.--Calibration Curve for Gage Six.

TABLE 7.1.--Values of Strain (ε) at Different Values of Load (N) for Gage Number 6

Load F (N)	Strain	Load F (N)	Strain
4.5	308	49.5	2390
9	606	54	2552
13.5	872	58.5	2686
18	1110	63	2804
22.5	1344	67.5	2920
27	1540	72	3018
31.5	1724	76.5	3118
36	1892	81	3210
40.5	2072	85.5	3310
45	2232	90	3410

Transducers were located at the proper points and were glued on the surface of the balls at the designated contact points. The contact points should seat exactly in the middle of the upper-plates of the transducers in order to obtain a correct force value. Three loading replications were made at each contact point considered. This process was completed for eight different transducer positions in the assemblage, Figure 7.8 a-h. The two top rows, 1 and 2, are added to the arrangement to create a uniform loading effect on the balls of row three and below. To locate the pressure transducer in Figure 7.8b, for example, the balls of the bottom row were carefully placed in the test box while the plexiglass window was removed. Then transducers were positioned and glued on the surface of the balls of the bottom row (layer 7) on the lower plate side of the transducer. Balls in the other rows were placed in a manner that it was made sure the balls were in contact at the right points. As the balls of the rows were placed and arranged from bottom to top, the plexiglass window was slided in piece by piece To reduce the friction between the balls and the sides of the test box, a lubricant (vaseline) was used.

7.4.2 Readjusting Digital Strain Indicator

Once the balls and the transducers for a particle arrangement were in palce, the test box was placed on the

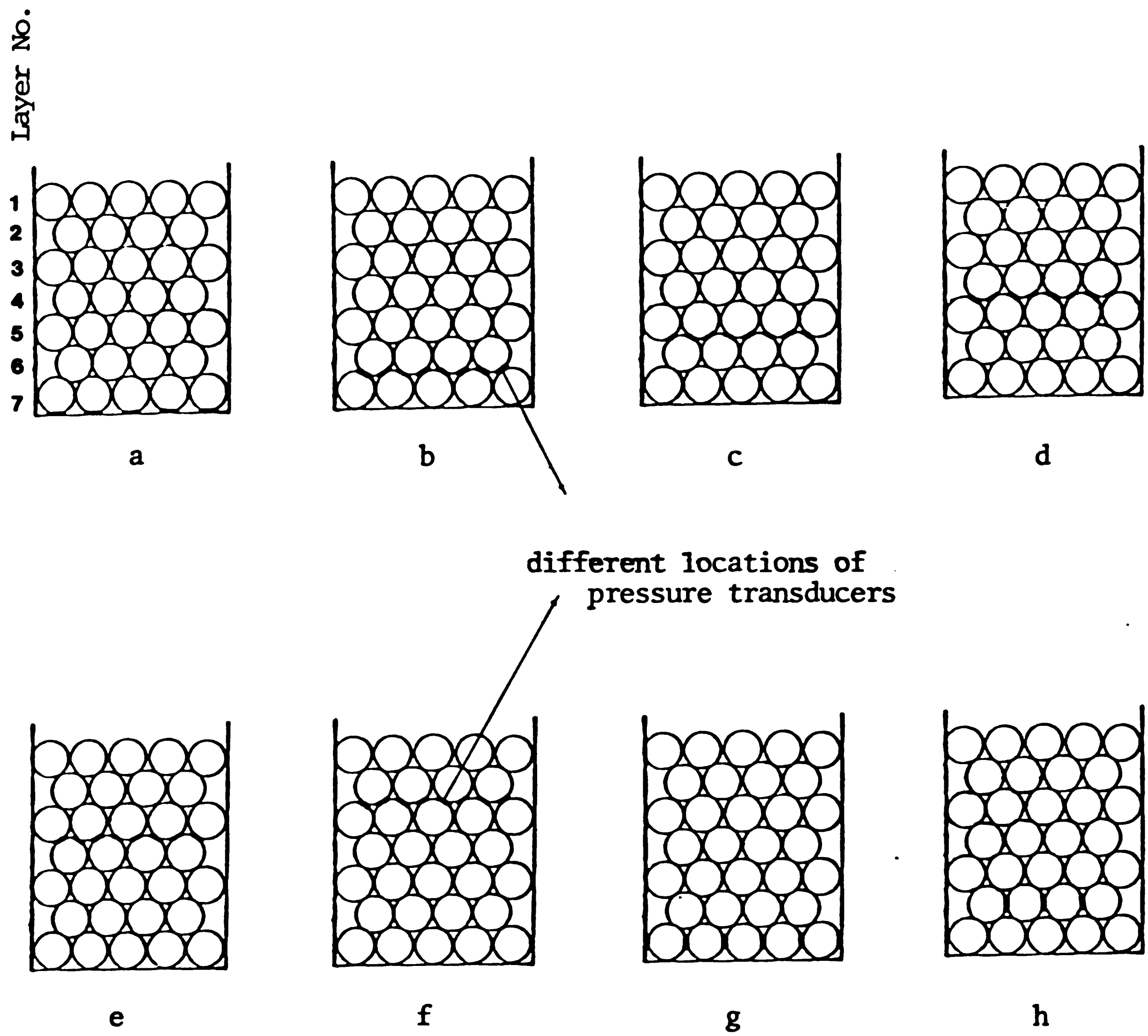

Figure 7.8.--Pressure Transducer Placement in Different Locations of the Assemblage.

load cell of the Instron and the initial strain resulting from the weight of the balls were removed by setting the strain indicator to zero.

7.4.3 Loading and Strain Reading

The load was applied using the Instron testing machine located in the Wood Technology Laboratory of the Forestry Department.

The Instron was zero balanced and the load was applied using a head speed of 0.508 cm/min (0.2 in/min). The Instron chart recorder was moving at 1.225 cm/min (0.5 in/min). Each location required about 12 minutes to print all the strain values. A maximum load of 202.5 N was applied. Strain values were printed every one-half minute and a mark was made on the loading curve of the Instron strip-chart recorder to indicate the corresponding load at that moment. The strain indicator printed one channel at the time with a two second time interval (20 seconds for all channels), Figure 7.9.

7.5 Results and Discussion

The measurement of the contact forces was replicated at least three times for each location and the average of these results are reported here. The contact forces were obtained for axial loads of 157.5, 180 and 202.5 N (35, 40 and 45 lbs). The applied forces and

Figure 7.9-- A Complete Set-Up of the Simulated Force Distribution Experiment of Two Dimensional Rhombohedral Arrangement of the Rubber Balls

correspoding strain values are given in Tables 7.2 through 7.4. Loads greater than 202.5 N were not applied because the pressure transducers were not as reliable in this loading range.

Corresponding planar graph of the applied loads are shown in Figures 7.10 through 7.12. For comparison between calculated and measured values of contact forces the planar graph representation of calculated contact forces are repeated in this section and are shown in Figures 7.13 through 7.15.

Comparing planar graph representation of calculated contact forces with the measured ones for three different loadings (157.5, 180 and 202.5 N) the following was concluded.

All the measured contact forces are within 20 percent of the calculated ones. A possible reason for this is that in the theory which was used to calculate the contact forces, the frictional forces were ignored. Actually there is friction between adjacent spheres and between the spheres and the walls of the test box. There is an approximate constant ratio of 1.14 between measured and calculated contact forces. If the frictional forces in the model were taken under consideration, then this constant ratio would be very small. In other words, the measured contact force values would be very close to the

Table 7.2--Average measured contact forces for 157.5 N of load

157.5 Newtons of Applied Load (31.5 Newtons on each Node)			
Channel No.	Ave. Observed Strain x 10^6	Ave. Measured Contact Forces (N)	Location of Transducers
0	1420	27.9	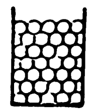
5	1560	27.9	
7	1582	27.9	
8	1668	27.9	
9	1520	27.9	
7	1150	18	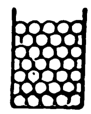
0	1040	18.45	
3	1050	18.45	
9	1200	20.7	
5	1230	20.25	
8	1200	18	
4	1150	18	
6	1100	17.55	
3	1050	18.45	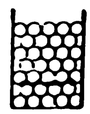
7	1140	17.55	
8	1380	21.6	
5	1050	16.65	
4	1070	17.1	
0	1180	21.6	
6	1100	17.55	
9	1100	18.45	
7	1170	18.45	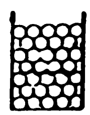
3	1390	26.1	
5	870	13.27	
4	1070	17.1	
0	960	16.65	
8	960	13.95	
9	1430	25.65	
6	1100	17.55	
7	1665	30.15	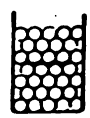
3	910	15.3	
5	980	15.3	
4	980	15.52	
0	885	15.07	
8	1040	15.3	
9	910	14.62	
6	1635	29.25	
0	9	0.22	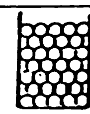
9	8	0.23	
3	4	0.21	
7	200	2.44	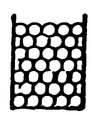
3	160	2.38	
4	215	2.38	
5	195	2.43	
0	290	3.94	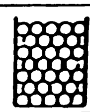
9	170	2.3	
3	265	3.92	

Table 7.3--Average measured contact forces for 180 N of load

180 Newtons of Applied Load (30 Newtons on each Node)			
Channel No.	Ave. Observed Strain x 10^6	Ave. Measured Contact Forces (N)	Location of Transducers
0 5 8 9 7	1530 1680 1792 1523 1512	30.6 31.o5 31.05 27.90 30.6	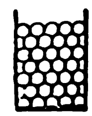
7 0 3 9 5 8 4 6	1280 1175 1150 1430 1390 1340 1250 1245	20.7 21.37 20.7 23.4 23.85 20.7 21.15 20.25	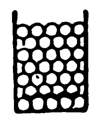
3 7 8 5 4 0 6 9	1155 1280 1550 1210 1180 1270 1245 1230	20.92 20.7 25.2 19.80 19.35 23.85 20.25 21.15	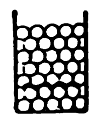
7 3 5 8 0 4 9 6	1280 1525 1020 1290 1080 990 1610 1280	20.7 29.47 16.2 19.8 19.35 15.52 30.15 21.15	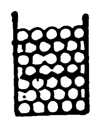
7 3 5 4 0 8 9 6	1805 950 1130 1100 980 1185 1000 1815	34.2 16.2 18.22 17.55 17.1 17.55 16.2 33.75	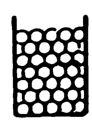
0 9 3	12 105 4	0.27 1.38 0.24	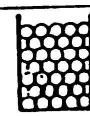
7 3 4 5	215 180 205 210	3 2.99 3.01 2.92	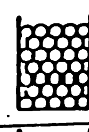
0 9 3	340 240 330	4.98 3.09 4.89	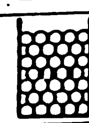

Table 7.4--Average measured contact forces for 202.5 N of load

202.5 Newtons of Applied Load (40.5 Newtons on each Node)			
Channel No.	Ave. Observed Strain x 10^6	Ave. Measured Contact Forces (N)	Location of Transducers
0 5 8 9 7	1574 1822 1911 1750 1849	31.95 35.1 34.2 33.75 35.55	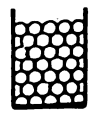
7 0 3 9 5 8 4 6	1360 1270 1310 1450 1500 1490 1370 1330	22.5 23.85 24.3 26.1 26.55 23.85 23.85 22.05	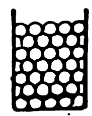
3 7 8 5 4 0 6 9	1290 1370 1685 1295 1280 1420 1365 1350	23.85 22.95 28.35 21.6 21.6 27.90 22.95 23.85	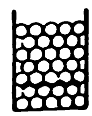
7 3 5 8 0 4 9 6	1400 1715 1080 1400 1180 1075 1725 1390	23.4 35.1 17.1 22.05 21.6 17.1 35.32 23.4	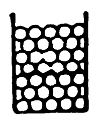
7 3 5 4 0 8 9 6	1965 1070 1250 1280 1180 1310 1200 2000	31.15 18.90 20.7 21.6 21.6 20.25 20.7 38.7	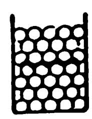
0 9 3	11 115 6	0.29 1.68 0.31	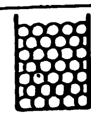
7 3 4 5	270 220 250 240	3.26 3.3 3.3 3.28	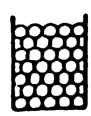
0 9 3	400 235 370	5.83 3.48 5.46	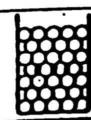

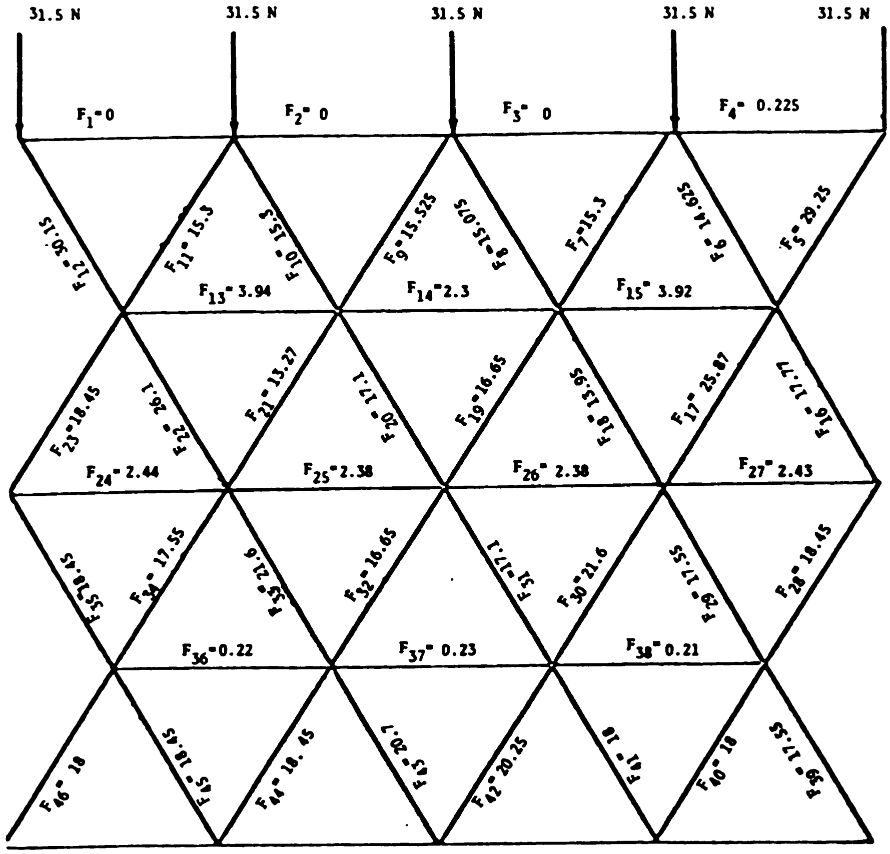

Figure 7.10.--Planar Graph Representation of Measured Contact Forces for a 157.5 N Load.

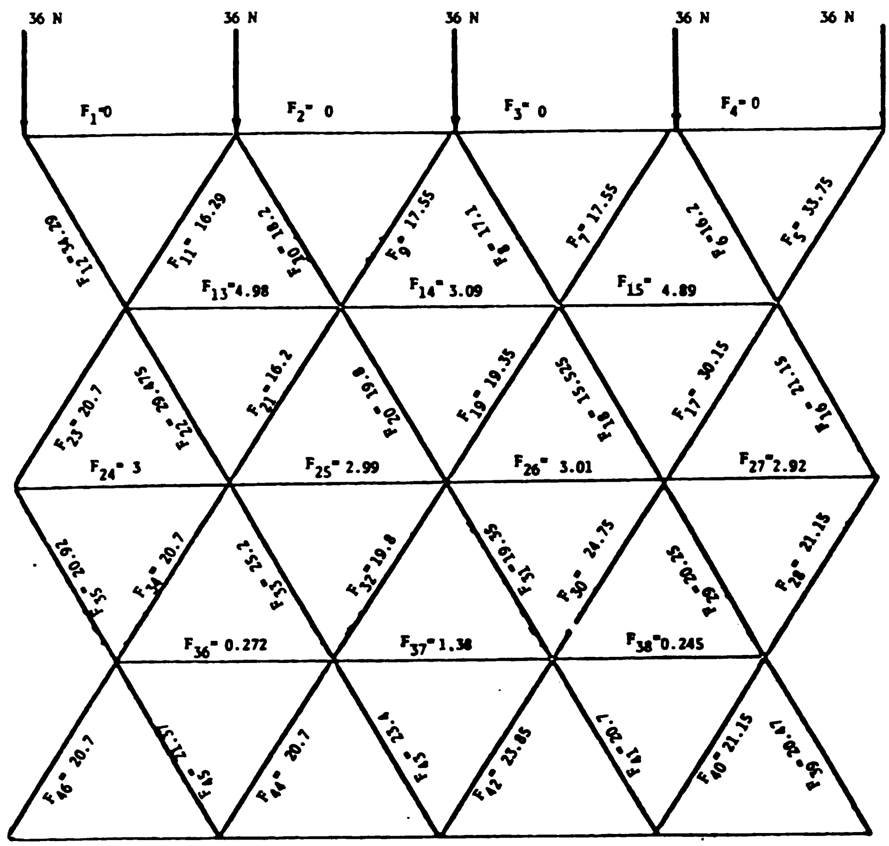

Figure 7.11.--Planar Graph Representation of Measured Contact Forces for a 180 N Load.

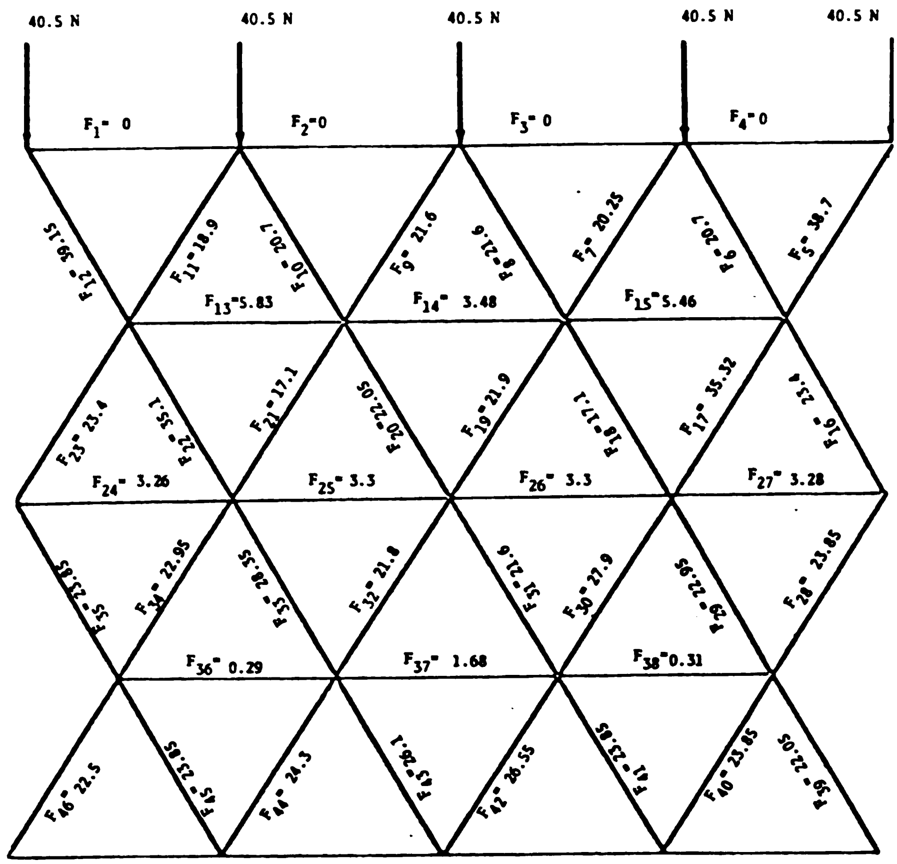

Figure 7.12.--Planar Graph Representation of Measured Contact Forces for a 202.5 N Load.

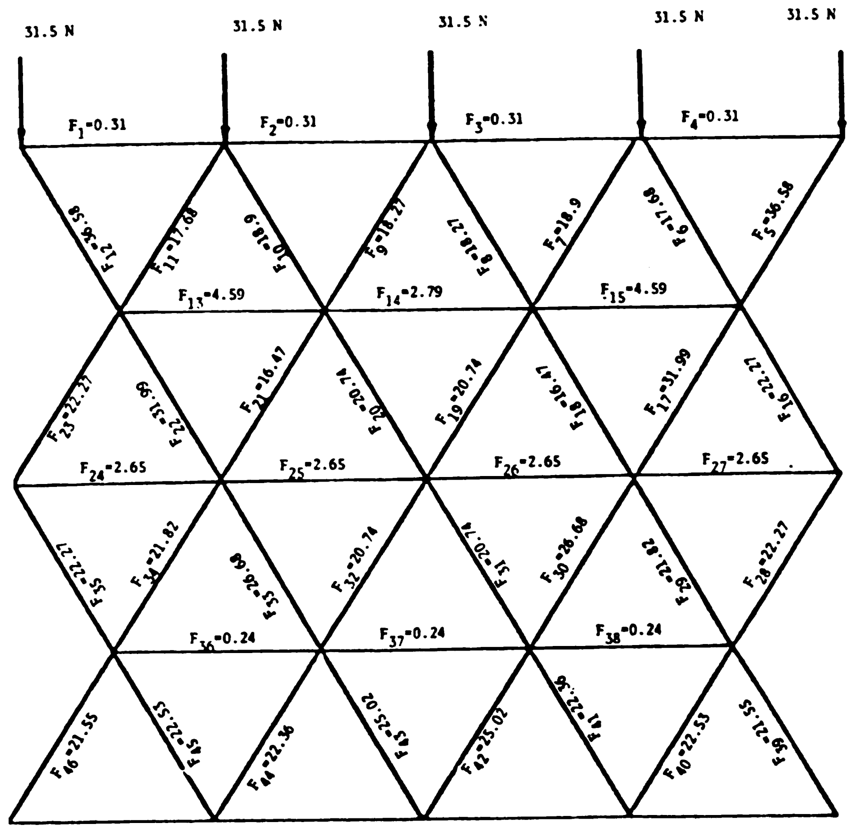

Figure 7.13.--Planar Graph Representation of Calculated Contact Forces for a 157.5 N Load. All Values in Newtons.

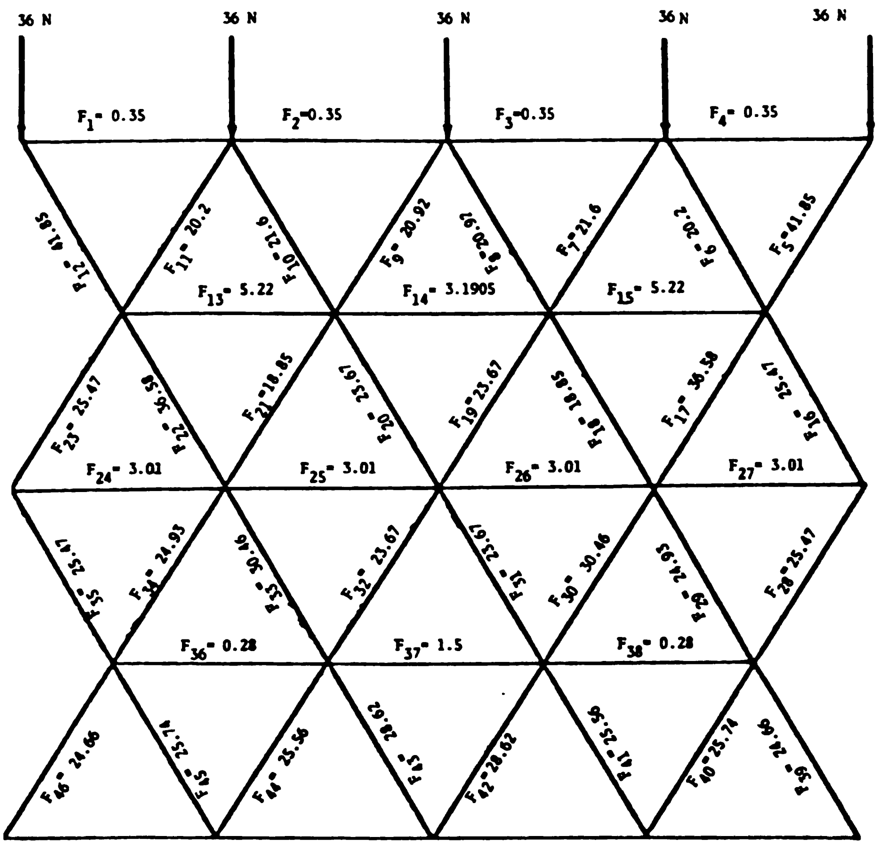

Figure 7.14.--Planar Graph Representation of Calculated Contact Forces for a 180 N Load. All Values in Newtons.

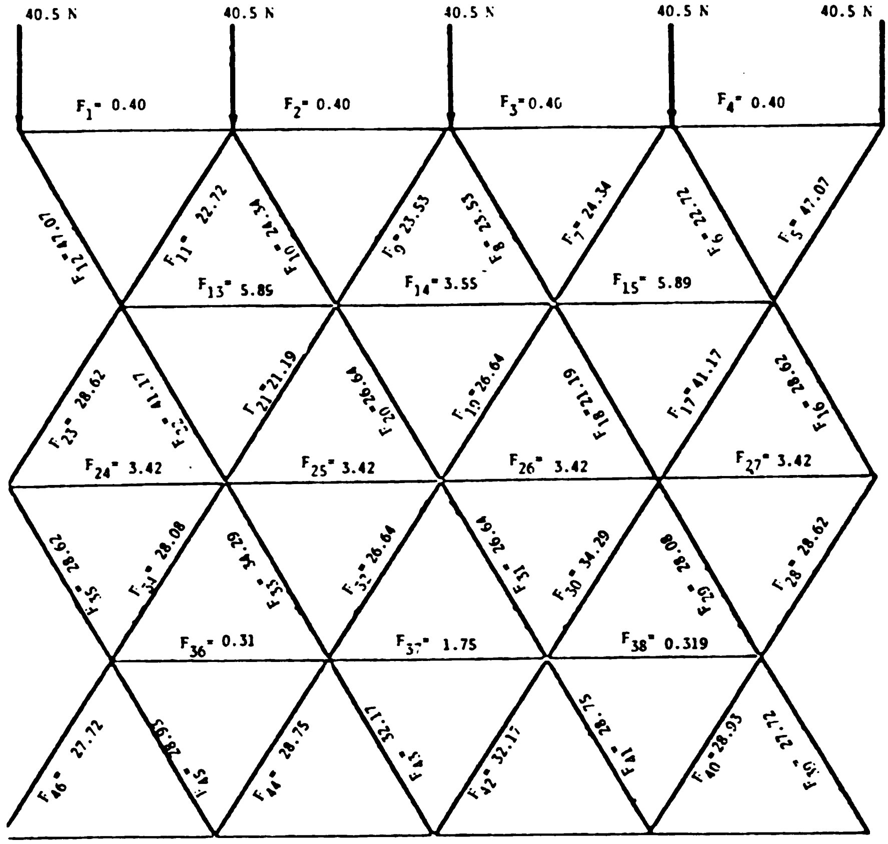

Figure 7.15.--Planar Graph Representation of Calculated Contact Forces for a 202.5 Load. All Values in Newtons.

calculated ones and error would be quite small. This indicates that the presented model could be more accurate than what was concluded earlier, if the frictional forces were considered.

The distribution of the contact forces in the members both in calculated and measured ones were very similar.

These will conclude that there is an agreement between the calculated values and the measured ones.

VIII. SUMMARY AND CONCLUSIONS

Development of experimental and analytical techniques to determine the maximum safe depth for apples in a bulk storage was the primary goal in this study. The problem was studied in two different components. One component involved the determination of the contact forces in a bulk bin while the other component related to the determination of whether a specific loading would produce a bruise.

Cylindrical specimens with a height of 1.27 cm and a diameter of 1.27 cm and a cross-sectional area of 1.266 cm^2 were prepared. These specimens were then compressed using a deformation rate of 1.27 cm per minute until a failure occurred. Tests were conducted on three different dates, October 1, November 15 and December 31. These were denoted as Groups I, II and III. Each group consisted of 150 apples and four samples were removed from each apple. The failure strain, ε_f, the stress at the failure, σ_f, and the elastic modulus, E, were determined for every sample. The modulus of elasticity changed significantly between October 1 and November 15. A much smaller change occurred between November 15 and

December 31. The respective averages were $E_{Oct} = 3279$ Kpa, $E_{Nov} = 2516$ Kpa and $E_{Dec} = 2360$ Kpa. The strain at failure showed a small decrease between October 1 and November 15. The reduction rate was lower between November 15 and December 31. The average maximum normal strain at failure was 0.14, 0.11 and 0.12 for the three dates. The average normal stress at failure decreased from 444 Kpa on October 1 to 252 Kpa on November 15 and 235 Kpa on December 31.

The distribution of the elastic modulus and failure strain were used in a computer model to predict bruising for a particular load. Since this model was based on the assumption that a bruise occurs when the maximum normal strain exceeds a specific value, an equation for the maximum normal strain was determined and used in a computer model.

The average location of the maximum normal strain for apple-to-apple contact was 3.65 mm for October first data and 3.0 mm for the other two sets of data. For apple in contact with a flat hard surface these values were 3.88 mm for October 1 data and 3.0 mm for the other two data.

To calculate the allowable storage depth, the modulus of elasticity of an apple in contact with another (E_1, E_2) and the failure strain of the pair of apples

(ε_{F1}, ε_{F2}) or apple in the case of flat plate contact were treated as random variables. A normal load F was selected and a random generator was used to select the values of E_1, E_2, ε_{F1} and ε_{F2} from the data obtained in the experimental part. The maximum strain in each apple was calculated. If this strain exceeded the failure strain for the apple, the apple was said to be bruised. The load which produced a bruise was converted to a depth by assuming a single column stack where each apple weighed 0.85 N.

Apple-to-apple contact was found to govern the allowable depth. The October 1 apples could be piled 5.14 meters without bruising but the November 15 and December 31 apples could be piled only about 1.8 meters. The significant decrease is due to the decrease in the modulus of elasticity between October 1 and November 15.

A finite element type computer model used for small diameter steel balls was modified for use with large diameter low modulus materials such as apples. This model is basically a two-dimensional truss analysis where the center of each sphere is considered as the node and the members connecting the nodes have the nonlinear property of two spheres in contact. The validity of the model was established by experimentally measuring the contact forces between 6 cm diameter rubber balls which were stacked in a rhombohedral fashion. Specially designed pressure transducers were located at the proper points and were glued on the surface of the balls in the assemblage. There were seven layers in the assemblage with either four or five balls in each horizontal layer. A maximum load of 202.5 N was applied by Instron and strain values were printed. All of the contact forces differed by less than 20 percent from the values calculated using the computer model.

The following conclusions were drawn from this study.

1. The maximum allowable height for freshly harvested Jonathan apples in contact with each other in a mono-column arrangement is 5.14 m (17.13 ft). This value decreases as the storage period increases. It was about 1.85 m (6.1 ft) after three months of storage at 2.2°C. As for apple in contact with a flat surface the maximum allowable safe depth was around 7 m for the October 1 apples and decreased to 2.2 m by November 15.

2. The modulus of elasticity of Jonathan apples decreased 23.3 percent between October 1, 1978, and November 15, 1978. The average of 600 samples was 3279 Kpa on October 1 and 2516 Kpa on November 15. The modulus value decreased another 6.2 percent between November 15 and December 21 to 2360 Kpa.

3. The failure strain of Jonathan apples averaged 0.14 on October 1, 1978, decreased to 0.11 on November 15 and then increased slightly to 0.12 by December 31.

4. The average failure stress of Jonathan apples decreased significantly between October 1 and December 31, 1978. It averaged 444 Kpa on October 1, 1978, and decreased to 252 Kpa by November 15 and further decreased to 235 Kpa by December 31. The total decrease of 209 Kpa was 47.1 percent of the original value.

5. The structural model formulation for calculating the contact forces within an arrangement of rubber balls disagreed with the experimental by a constant ratio. The experimental results were about 0.83 of the calculated values.

6. The susceptibility of two apples in contact to bruising is higher than that of an apple in contact with a rigid flat surface because maximum allowable safe depth for any of three groups of apples in Case II (apple in contact with rigid flat surface) was always higher than Case I (two apples in contact).

IX. SUGGESTIONS FOR FUTURE RESEARCH

Suggestions for future research based on the experiences and results of this study include:

1. The significant variation of the mechanical properties of Jonathan apples during the first 1.5 months of storage indicates that these properties should be studied on a weekly basis or at least every two weeks.

2. Allowable depth values should be calculated for other varieties of apples which may be stored in bulk, These calculations cannot be performed without the distributions of the mechanical properties thus these properties must be studied as a function of storage time.

3. The presence of skin was neglected in this investigation and apples were assumed to be an isotropic, homogeneous mass. Rumsey and Fridley (1974) found that the presence of an elastic skin produced no significant change of the internal stress distribution. Gustafson (1974), however, showed that the restraint created by the skin can cause increased stresses in the body if the turgor pressure is accounted for. The effect of skin properties on the maximum allowable contact force from one apple to another or from the apple to a rigid flat

surface, however, has to be investigated. Consideration of apple skin and core might lead to dealing with anisotropic materials, which in reality is considering the whole apple not just one part of it.

4. The measurement of strain at failure under numerous deformation rates.

APPENDICES

APPENDIX A

EXPERIMENTAL DATA

TABLE A.1.--Mean Values of the Three Different Parameters (ε_f, σ and E)--Group I

Date : Oct 1, 1978 (Group I)
Variety : Jonathan
Head Speed of Instron : 1.27 Cm/min
Chart Speed : 25.4 Cm/min

Sample Height : 1.27 Cm
Sample Diameter : 1.27 Cm
Sample Cross-section Area : 1.266 Cm^2

Apple No.	ε_{FA}	σ_{FA} (Kpa)	E_A (Kpa)	Apple No.	ε_{FA}	σ_{FA} (Kpa)	E_A (Kpa)	Apple No.	ε_{FA}	σ_{FA} (Kpa)	E_A (Kpa)	Apple No.	ε_{FA}	σ_{FA} (Kpa)	E_A (Kpa)
1	0.140	476.06	3528.97	41	0.15	453.42	3144.85	81	0.148	417.43	3000.52	121	0.143	448.00	3302.30
2	0.148	427.68	3048.02	42	0.144	455.74	3474.35	82	0.138	405.43	3019.34	122	0.149	463.81	3678.26
3	0.140	470.83	3713.83	43	0.151	470.45	3312.19	83	0.138	428.07	3182.77	123	0.153	453.78	3194.04
4	0.144	451.29	3443.49	44	0.146	492.37	3783.65	84	0.150	453.03	3262.02	124	0.147	371.56	3111.96
5	0.147	431.16	3081.01	45	0.150	443.74	3292.57	85	0.145	415.10	3117.08	125	0.160	526.38	3706.14
6	0.145	429.23	3096.63	46	0.150	465.78	3336.76	86	0.152	453.23	3239.8	126	0.157	441.23	3075.39
7	0.134	434.84	3453.68	47	0.146	506.83	3900.24	87	0.146	442.2	3452.48	127	0.153	459.61	3373.17
8	0.145	526.76	4259.15	48	0.153	448.97	3115.37	88	0.152	436.39	3451.07	128	0.163	522.45	3478.11
9	0.150	432.29	3234.06	49	0.163	416.71	2684.34	89	0.162	478.00	3170.93	129	0.162	469.24	3224.50
10	0.150	456.32	3544.02	50	0.136	439.10	3353.12	90	0.148	447.02	3469.38	130	0.145	455.71	3495.63
11	0.147	447.23	3492.96	51	0.154	419.39	3063.90	91	0.151	409.30	2990.99	131	0.148	412.16	3057.47
12	0.137	448.50	3520.85	52	0.138	453.62	3523.46	92	0.158	510.90	3487.77	132	0.157	382.16	2605.50
13	0.159	439.87	2842.89	53	0.154	425.75	3141.25	93	0.148	464.45	3273.91	133	0.150	424.75	3027.36
14	0.140	403.11	3112.12	54	0.148	484.19	3653.93	94	0.160	428.65	2950.33	134	0.147	409.30	3008.24
15	0.140	453.23	3560.57	55	0.148	424.39	3109.03	95	0.148	450.50	3441.33	135	0.162	480.90	3178.79
16	0.139	451.48	3478.90	56	0.145	472.77	3686.52	96	0.142	463.48	3341.37	136	0.153	461.54	3313.22
17	0.146	431.55	3155.89	57	0.146	449.16	2717.82	97	0.137	418.39	3169.96	137	0.160	443.16	3265.93
18	0.129	423.04	3371.31	58	0.147	440.65	3196.05	98	0.150	458.05	3359.40	138	0.155	455.74	3222.45
19	0.146	463.68	3508.34	59	0.148	415.49	3103.42	99	0.151	423.17	3229.33	139	0.153	436.39	3135.51
20	0.138	453.42	3540.18	60	0.143	408.33	3155.89	100	0.151	445.48	3236.18	140	0.145	432.52	3282.56
21	0.149	490.38	3568.23	61	0.147	473.55	3400.27	101	0.147	407.34	3247.41	141	0.146	415.10	3122.08
22	0.148	465.23	3423.26	62	0.143	467.44	3522.28	102	0.162	424.78	3186.28	142	0.144	468.32	3412.51
23	0.144	462.32	3532.53	63	0.153	431.03	3089.14	103	0.142	456.71	3393.92	143	0.145	478.97	3714.24
24	0.144	445.29	3297.57	64	0.151	450.85	3175.97	104	0.166	394.78	2843.71	144	0.146	462.50	3344.71
25	0.163	491.93	3232.02	65	0.159	471.22	3226.03	105	0.151	477.03	3483.74	145	0.161	466.39	3260.06
26	0.141	470.44	3576.53	66	0.153	469.10	3247.92	106	0.146	383.17	3117.20	146	0.151	448.97	3113.30
27	0.140	472.39	3755.21	67	0.141	404.45	3110.45	107	0.150	430.34	2976.19	147	0.153	441.94	3052.15
28	0.156	476.52	3364.4	68	0.146	411.43	3258.69	108	0.143	349.50	2949.75	148	0.137	456.69	3546.30
29	0.152	456.90	4256.27	69	0.146	423.81	3190.62	109	0.153	418.96	3121.02	149	0.143	403.49	2991.45
30	0.153	460.58	3182.95	70	0.140	425.73	3150.19	110	0.145	440.26	3507.10	150	0.150	433.49	3214.43
31	0.152	450.50	3186.36	71	0.141	441.42	3358.16	111	0.151	392.84	2972.82				
32	0.148	399.43	2944.23	72	0.151	463.29	3157.83	112	0.155	477.99	3507.06				
33	0.143	441.81	3207.90	73	0.148	460.77	3159.80	113	0.141	403.49	3161.03				
34	0.148	439.68	3253.27	74	0.151	420.90	2952.00	114	0.143	412.20	3024.48				
35	0.150	424.58	3807.18	75	0.154	446.84	3122.30	115	0.147	382.58	3400.55				
36	0.148	430.97	3265.71	76	0.161	439.87	2981.56	116	0.150	411.23	3117.32				
37	0.143	520.77	4043.57	77	0.151	434.46	3087.90	117	0.155	433.48	3354.16				
38	0.151	427.68	3205.80	78	0.138	392.65	2945.95	118	0.147	407.75	3144.50				
39	0.150	456.32	3274.89	79	0.146	465.40	3366.23	119	0.145	392.65	2950.50				
40	0.143	440.13	3362.80	80	0.148	484.77	3699.15	120	0.147	431.92	3321.96				

TABLE A.2.--Mean Values of the Three Different Parameters (ε_f, σ, and E)--Group II

Date : Nov 15, 1978 (Group II)
Variety : Jonathan
Head Speed of Instron : 1.27 Cm/min
Chart Speed : 25.4 Cm/min

Sample Height : 1.27 Cm
Sample Diameter : 1.27 Cm
Sample Cross-section area : 1.266 Cm^2

Apple No.	ε_{FA}	σ_{FA} (Kpa)	E_A (Kpa)	Apple No.	ε_{FA}	σ_{FA} (Kpa)	E_A (Kpa)	Apple No.	ε_{FA}	σ_{FA} (Kpa)	E_A (Kpa)	Apple No.	ε_{FA}	σ_{FA} (Kpa)	E_A (Kpa)
1	0.115	258.35	2867.15	41	0.121	248.68	2506.14	81	0.125	243.84	2486.79	121	0.116	250.61	2457.76
2	0.116	271.90	3252.83	42	0.121	239.97	2296.49	82	0.120	226.42	2167.48	122	0.130	292.22	2464.21
3	0.096	241.90	2914.60	43	0.123	253.51	2670.64	83	0.108	227.39	2409.38	123	0.123	202.23	2238.43
4	0.112	297.06	3206.06	44	0.121	269.96	2534.25	84	0.113	236.10	2338.42	124	0.134	270.93	2644.38
5	0.115	249.64	2502.92	45	0.119	248.68	2429.20	85	0.111	222.55	2032.01	125	0.133	249.64	2206.18
6	0.113	254.16	2644.84	46	0.118	239.97	2406.16	86	0.123	240.93	2270.69	126	0.121	261.25	2451.31
7	0.147	323.18	2640.54	47	0.110	271.90	2673.87	87	0.110	216.74	2183.60	127	0.128	267.06	2515.82
8	0.117	308.67	3119.59	48	0.120	316.41	2808.92	88	0.116	245.77	2290.45	128	0.121	228.36	2219.08
9	0.118	276.74	3031.88	49	0.125	238.03	2125.55	89	0.116	229.32	2306.17	129	0.104	212.87	2353.63
10	0.117	275.77	2919.00	50	0.119	278.67	2757.73	90	0.105	233.19	2509.37	130	0.123	239.97	2115.87
11	0.112	274.80	2773.85	51	0.113	257.38	2831.91	91	0.115	244.80	2535.17	131	0.126	224.48	2156.42
12	0.116	302.86	3193.16	52	0.118	223.52	2164.25	92	0.114	223.52	2244.89	132	0.116	265.12	2725.47
13	0.115	303.83	3048.01	53	0.108	234.16	2459.76	93	0.126	233.19	2090.07	133	0.129	230.29	2154.57
14	0.107	287.38	3096.40	54	0.113	306.73	3067.37	94	0.108	241.90	2451.31	134	0.123	262.22	2599.91
15	0.123	245.77	2560.98	55	0.116	284.48	2878.68	95	0.094	243.84	3096.40	135	0.124	242.87	2238.43
16	0.125	291.25	2924.07	56	0.109	290.28	2862.55	96	0.121	235.13	2273.91	136	0.125	256.42	2361.00
17	0.111	291.55	3077.04	57	0.119	285.44	2626.41	97	0.113	232.23	2341.66	137	0.135	245.77	2061.04
18	0.114	249.61	2574.34	58	0.121	262.22	2486.79	98	0.118	249.64	2399.71	138	0.111	204.16	2118.63
19	0.126	297.06	2739.30	59	0.133	195.46	1699.79	99	0.100	220.61	2467.44	139	0.128	214.81	2051.36
20	0.123	322.21	2955.01	60	0.121	227.39	2144.90	100	0.120	265.12	2464.21	140	0.120	252.55	2361.00
21	0.100	214.80	2372.06	61	0.113	248.6	2454.54	101	0.111	247.71	2409.38	141	0.124	226.42	2181.76
22	0.118	246.74	2528.72	62	0.113	229.32	2215.40	102	0.113	231.26	2298.10	142	0.129	250.61	2425.50
23	0.113	257.38	2738.37	63	0.108	252.55	2496.47	103	0.118	205.13	2051.36	143	0.125	235.13	2148.12
24	0.125	259.32	2305.71	64	0.106	248.68	3141.55	104	0.125	290.28	2902.87	144	0.145	260.29	2315.84
25	0.120	266.09	2443.25	65	0.121	269.96	2406.16	105	0.108	227.39	2386.80	145	0.135	263.19	2352.71
26	0.133	281.57	2354.55	66	0.118	243.84	2317.46	106	0.106	243.84	2580.33	146	0.138	254.48	2354.55
27	0.114	239.00	2696.44	67	0.127	247.71	2225.53	107	0.118	254.48	2419.06	147	0.128	248.68	2379.18
28	0.129	311.57	2823.62	68	0.113	244.80	2361.00	108	0.123	223.52	2061.04	148	0.126	221.58	2161.02
29	0126	237.06	2113.56	69	0.128	270.93	2419.06	109	0.125	241.90	2277.14	149	0.133	231.45	2302.94
30	0.125	275.77	2509.37	70	0.111	219.65	2273.91	110	0.109	231.26	2457.76	150	0.139	251.58	2115.74
31	0.114	282.54	2846.43	71	0.113	249.64	2346.49	111	0.124	219.65	2080.39				
32	0.119	285.44	2889.97	72	0.118	278.67	2609.36	112	0.125	238.03	2151.35				
33	0.119	251.58	2788.37	73	0.104	276.74	3028.66	113	0.115	262.22	2657.74				
34	0.118	222.55	2161.02	74	0.116	231.26	2219.08	114	0.120	248.68	2509.37				
35	0.121	325.12	2994.79	75	0.120	263.19	2541.62	115	0.124	250.61	2247.65				
36	0.121	267.06	2515.82	76	0.113	256.42	2660.96	116	0.131	228.36	2115.87				
37	0.105	270.93	3212.51	77	0.126	233.19	2157.80	117	0.123	226.42	2212.63				
38	0.125	248.68	2222.08	78	0.121	230.29	2132.92	118	0.121	224.48	2112.64				
39	0.113	210.94	2075.99	79	0.113	239.48	2396.48	119	0.125	266.09	2477.12				
40	0.119	310.6	2967.38	80	0.111	256.42	2612.58	120	0.114	217.71	2264.24				

TABLE A.3.--Mean Values of the Three Different Parameters (ε_f, σ, and E)--Group III

Date	:Dec 30, 1978 (Group III)	Sample Height	: 1.27 Cm
Variety	: Jonathan	Sample Diameter	: 1.27 Cm
Head Speed of Instron	: 1.27 Cm/min	Sample Cross-section area	: 1.266 Cm^2
Chart Speed	: 25.4 Cm/min		

Apple No.	ε_{FA}	σ_{FA} (Kpa)	E_A (Kpa)	Apple No.	ε_{FA}	σ_{FA} (Kpa)	E_A (Kpa)	Apple No.	ε_{FA}	σ_{FA} (Kpa)	E_A (Kpa)	Apple No.	ε_{FA}	σ_{FA} (Kpa)	E_A (Kpa)
1	0.124	270.45	2443.24	41	0.138	274.80	2603.62	81	0.141	208.52	1915.27	121	0.121	234.06	2412.15
2	0.130	220.03	2242.24	42	0.124	228.74	2139.83	82	0.121	271.41	2706.27	122	0.128	229.81	2262.39
3	0.121	199.81	2056.20	43	0.109	253.90	2552.68	83	0.130	188.97	2381.04	123	0.129	216.74	2438.26
4	0.105	219.65	2556.14	44	0.129	202.23	2073.22	84	0.121	223.90	2184.95	124	0.134	229.81	2550.22
5	0.135	240.84	2180.38	45	0.121	230.68	2290.68	85	0.128	262.71	2641.25	125	0.121	224.00	2583.55
6	0.124	240.45	2162.64	46	0.133	221.10	2026.36	86	0.123	252.55	2577.10	126	0.120	234.64	2484.72
7	0.123	200.87	2161.02	47	0.116	258.84	3019.60	87	0.124	241.42	2434.95	127	0.135	240.93	2631.01
8	0.125	207.07	2019.11	48	0.121	209.97	2052.74	88	0.110	283.51	3096.40	128	0.115	241.90	2741.60
9	0.120	201.76	1949.76	49	0.130	233.00	2102.63	89	0.131	205.13	2077.32	129	0.121	216.74	2333.77
10	0.143	234.46	2038.48	50	0.126	223.03	2297.82	90	0.121	225.84	2409.23	130	0.135	244.03	2532.41
11	0.113	209.39	1911.05	51	0.120	222.55	2380.35	91	0.119	201.65	2061.77	131	0.131	228.84	2218.62
12	0.125	233.68	2006.20	52	0.118	264.16	2589.08	92	o.120	231.64	2519.28	132	0.120	190.62	2411.25
13	0.116	233.98	2136.83	53	0.118	285.44	2733.54	93	0.125	216.74	2273.15	133	0.111	235.67	2609.36
14	0.125	194.49	1902.99	54	0.120	239.97	2429.04	94	0.124	222.55	2303.86	134	0.111	195.46	2068.29
15	0.136	229.71	1957.44	55	0.120	244.32	2407.54	95	0.125	218.68	2322.00	135	0.125	250.13	2525.04
16	0.138	225.94	2068.29	56	0.119	220.42	2280.95	96	0.134	230.19	2182.91	136	0.124	248.19	2773.85
17	0.120	229.23	2128.77	57	0.124	251.87	2546.04	97	0.125	241.32	2451.31	137	0.131	268.51	2482.03
18	0.125	268.41	2335.20	58	0.116	245.77	2999.63	98	0.130	237.06	2410.99	138	0.139	283.32	2921.48
19	0.118	246.74	2185.22	59	0.125	243.35	2113.80	99	0.125	262.71	2584.88	139	0.136	206.58	2135.22
20	0.118	220.61	2215.86	60	0.124	260.29	2563.68	100	0.125	217.23	2414.58	140	0.129	195.99	1998.99
21	0.125	213.89	1858.64	61	0.121	214.81	2096.52	101	0.130	232.71	2318.84	141	0.121	214.81	2130.56
22	0.121	195.46	2075.55	62	0.125	237.06	2483.57	102	0.128	219.16	2292.47	142	0.114	218.19	2528.72
23	0.126	164.98	1678.82	63	0.120	266.09	2882.14	103	0.138	255.93	2455.54	143	0.126	234.16	2489.33
24	0.124	224.19	2197.31	64	0.128	239.00	2267.46	104	0.124	239.00	2603.37	144	0.125	241.90	2516.74
25	0.124	261.16	2477.92	65	0.121	235.61	2459.38	105	0.131	251.00	2403.70	145	0.129	244.32	2591.62
26	0.130	237.55	2386.80	66	0.131	252.55	2559.59	106	0.134	264.16	2538.86	146	0.136	239.97	2607.05
27	0.130	217.13	2179.26	67	0.136	291.25	2716.90	107	0.125	236.39	2361.46	147	0.125	239.97	2689.99
28	0.124	209.49	1969.80	68	0.120	222.07	2303,86	108	0.131	211.91	2175.42	148	0.115	231.26	2791.98
29	0.140	221.58	2028.78	69	0.131	243.84	2393.56	109	0.128	209.97	2235.24	149	0.125	275.77	2912.55
30	0.141	253.51	2685.15	70	0.120	238.03	2491.63	110	0.128	234.16	2295.36	150	0.120	199.33	2004.36
31	0.120	228.74	2289.12	71	0.121	229.81	2305.26	111	0.118	236.10	2690.91				
32	0.145	245.96	2478.96	72	0.116	224.48	2332.78	112	0.119	221.58	2509.37				
33	0.118	240.93	2483.57	73	0.126	287.86	2890.43	113	0.111	247.71	2659.68				
34	0.124	231.46	2092.48	74	0.128	259.80	2502.51	114	0.129	232.23	2394.58				
35	0.149	230.77	2061.57	75	0.129	254.00	2554.53	115	0.126	250.03	2589.54				
36	0.133	229.81	2239.36	76	0.120	252.55	2451.31	116	0.109	215.58	2316.78				
37	0.136	243.84	2148.74	77	0.128	255.93	2422.67	117	0.123	203.68	2083.54				
38	0.129	245.58	2179.56	78	0.129	242.87	2522.73	118	0.135	214.32	2153.92				
39	0.129	211.32	2013.98	79	0.123	230.29	2488.17	119	0.131	249.64	2518.40				
40	0.129	241.90	1981.51	80	0.115	223.03	2540.01	120	0.118	209.97	2105.16				

APPENDIX B

COMPUTER PROGRAM FOR CALCULATION OF HEIGHT AND PERCENT BRUISE RELATIONSHIP

Computer Program for Calculation of Height and Percent Bruise Relation-ship, Case I, Group I :

```
      PROGRAM ORDER(INPUT,OUTPUT,TAPE5=INPUT,TAPE6=OUTPUT)
      DIMENSION E(150),EPS(150)
C E = IS THE MODULUS OF ELASTICITY.
C EPS = IS THE FAILURE STRAIN.
      READ(5,*)  (E(I),I=1,150), (EPS(I), I=1,150)
      DO 200 N=25,150,1
      RN=N*1.0E-6
      ICOUNT=0
      PRINT *,RN
      DO 100 J=1,500
      Y1=RANF(-1)   $   Y2=RANF(-1)
      I1=149.999*Y1+1   $   I2=149.999*Y2+1
      E1=E(I1)  $  EPS1=EPS(I1)
      E2=E(I2)  $   EPS2=EPS(I2)
      E11=((E1+E2)/(E1*E2))
      C1=.07333*E1*E11**(2./3.)*RN**(-1./3.)
      C2=.07333*E2*E11**(2./3.)*RN**(-1./3.)
      A11=RN**(-1./3.)*E11**(-1./3.)
      A22=RN**(1./3.)*E11**(1./3.)
      B11=RN**(-2./3.)*E11**(-2./3.)
      AA=35.59
      Z=AA*1.0E-4
      A=4.599*Z*A11*ATAN(.21749*(1./Z)*A22)
      B=1./(1.+21.1416*Z**(2.)*B11)
      EPSMAX1=ABS(.7/C1*(1.-A)-B/C1)
      EPSMAX2=ABS(.7/C2*(1.-A)-B/C2)
      IF (EPSMAX1 .LT. EPS1) GO TO 50
      ICOUNT=ICOUNT+1
   50 IF (EPSMAX2.LT.EPS2) GO TO 100
      ICOUNT=ICOUNT+1
  100 CONTINUE
      PERCENT=ICOUNT/10.
  200 PRINT*,PERCENT
      END
```

Computer Program for Calculation of Height and percent Bruise Relation-ship, Case II, Group I :

```
      PROGRAM ORDER(INPUT,OUTPUT,TAPE5=INPUT,TAPE6=OUTPUT)
      DIMENSION F(150),EPS(150)
      READ(5,*)  (F(I),I=1,150), (EPS(I), I=1,150)
      DO 200 N=80,150
      RN=N*1.0E-6
      ICOUNT=0
      PRINT *,RN
      DO 100 I=1,150
      Y2=RANF(-1)
      I2=149.999*Y2+1
      F2=F(I2)       $      EPS2=EPS(I2)
      A=(RN*(1715277.769+8.5995*F2)/(8274.0(0.0+F2))**(1./3.)
      PC=(.47746483*RN)/(A**(2.))
      AA=38.83
      Z=AA*1.0E-4
      C=Z/A
      EPSMAX2=ABS((1./F2)*((1.35)*PC)*(.7*(1.-C*ATAN(1./C))-1./(1.+C**
     12.))))
      IF (EPSMAX2.LT.EPS2) GO TO 100
      ICOUNT=ICOUNT+1
  100 CONTINUE
      PERCENT=(ICOUNT)*(100.)/(150.)
  200 PRINT*,PERCENT
      END
```

APPENDIX C

A COMPUTER PROGRAM FOR CALCULATION OF CONTACT FORCES AND NODAL DEFLECTIONS IN A TWO DIMENSIONAL RHOMBOHEDRAL ASSEMBLAGE OF SPHERES

APPENDIX C

A COMPUTER PROGRAM FOR CALCULATION OF CONTACT FORCES AND NODAL DEFLECTIONS IN A TWO DIMENSIONAL RHOMBOHEDRAL ASSEMBLAGE OF SPHERES

The following computer program was written in the basic language for the CDC 6500 to solve Equation (6.6). The given data are the transformation matrix [N] = (32 x 50) and the force matrix {P} = (32 x 1). The program compares the contact forces as well as nodal deflections after each iteration with those calculated previously to determine when to half the solution. The covergence to the solution was obtained when both contact forces and nodal deflections after each iteration with those calculated previously to determine when to halt the solution. The convergence to the solution was obtained when both contact forces and nodal deflections had the same last three decimal points and it was achieved in the 18th iteration.

```
100BASE1
110DIM E(32,50),A1(32,50),B(50,50),C(50,32),F(32,32),G(50),F1(32,32)
120DIM P(32),D(32),F2(50),M(50)
130DIMQ(50,50)
140MARGIN 132
150SETDIGITS 5
160MAT Q=IDN(50,50)
170MAT B=(-39.44)*Q
180MAT READ A1
190PRINT "A1"
200REMMAT PRINT A1;
210MAT READ P
220PRINT"P"
230REMMAT PRINT P;
240J=1
250MAT C=TRN(A1)
260PRINT "C(";J;")"
270REMMAT PRINT C;
280MAT E=A1*B
290PRINT "E(";J;")"
300REMMAT PRINT E;
310MAT F=E*C
320PRINT "F(";J;")"
330REMMAT PRINT F;
340MAT F1=INV(F)
350PRINT "F1(";J;")"
360REMMAT PRINT F1;
370MAT D=F1*P
380IF INT(J/3)<> J/3 THEN 410
390PRINT"D(";J;")"
400MAT PRINT D;
410MAT G=C*D
420FOR I=1TO50
430F2(I)=78.26*SQR(ABS(G(I)**3))
440NEXT I
450IF INT(J/3)<> J/3 THEN490
460PRINT "F2(";J;")"
470MAT PRINT F2;
480PRINT"G(";J;")"
490REMMAT PRINT G;
500FOR I=1TO50
510B(I,I)=78.26*SQR(ABS(G(I)))
520NEXT I
530PRINT "B(";J;")"
540REMMAT PRINT B;
550J=J+1
560GO TO 250
570REM NOTHING
```

APPENDIX D

CALCULATION OF LOCATION OF MAXIMUM STRAIN (Z) IN A SINGLE APPLE UNDER CONTACT LOAD

APPENDIX D

CALCULATION OF LOCATION OF MEXIMUM STRAIN (Z) IN A SINGLE APPLE UNDER CONTACT LOAD

Case I: Two Apples in Contact

In this case two apples are in contact with two different modulii of elasticity, E_1 and E_2. Measured values of strain at failure (ε_f) and the modulus of elasticity of 150 apples were used to determine the depth at which the maximum strain occurs (Z).

The following computer program calculates the value of Z for different loads (F). The program is set up in such a way that each time two modulus of elasticity values and their coupled corresponding strains at failure is randomly chosen (out-off 150 available data for each testing date. This is done by RANF (-1) in the program). Substituting randomly chosen E_1 and E_2 in the place of E in Equation 5.2 will give ε_{max1} and ε_{max2}, respectively. The program compares these two values (calculated maximum strain at failure) with the actual (measured) values of strain at failure and counts the value of calculated strain if it is larger than the measured one. This process is repeated for different depth (Z) from 0.1 mm up to 5 mm. Each time maximum strain and its corresponding Z value under a given load (F) will be printed.

Figure 5.1 shows the relation between depth (Z) and maximum strain ε_{max} under different loads (F). It was found that the maximum strain for apples group I occurs around Z = 3.56 mm and for group II and III it is around Z = 3.0 mm.

Computer Program for Calculation of Z in Case I, Group I :

```
      PROGRAM [illegible](INPUT,OUTPUT,TAPE5=INPUT,TAPE6=OUTPUT)
      DIMENSION E(150),EPS(150)
C E = IS THE MODULUS OF ELASTICITY.
C EPS = IS THE FAILURE STRAIN.
      READ(5,*)  (E(I),I=1,150), (EPS(I), I=1,150)
      DO 200 N=5[illegible],16[illegible]
      RN=N*1.E-6
      PRINT 2,N
    2 FORMAT(*1N=*,I5)
      DO 100 I=1,1[illegible]
      Y1=RANF(-1)  $  Y2=RANF(-1)
      I1=149.999*Y1+1  $  I2=149.999*Y2+1
      E1=E(I1)  $  EPS1=EPS(I1)
      E2=E(I2)  $  EPS2=EPS(I2)
      E11=((E1+E2)/(E1*E2))
      C1=.7[illegible]3*E1*E11**(2./3.)*RN**(-1./3.)
      C2=.7[illegible]3*E2*E11**(2./3.)*RN**(-1./3.)
      A11=RN**(-1./3.)*E11**(-1./3.)
      A22=RN**(1./3.)*E11**(1./3.)
      B11=RN**(-2./3.)*E11**(-2./3.)
      DO 300 II=1,50
      Z=II*1.0E-4
      A=4.599*Z*A11*ATAN(.21742*(1./Z)*A22)
      B=1./(1.+21.1416*Z**(2.)*B11)
      EPSMAX1=ABS(.7/C1*(1.-A)-B/C1)
      EPSMAX2=ABS(.7/C2*(1.-A)-B/C2)
      IF (EPSMAX1 .LT. EPS1) GO TO 50
      PRINT 3,II,EPSMAX1
    3 FORMAT(* II=*,I3,3X,*EPSMAX1=*,F10.3)
   50 IF (EPSMAX2.LT.EPS2) GO TO 300
      PRINT 4,II,EPSMAX2
    4 FORMAT(* II=*,I3,3X,*EPSMAX2=*,F10.3)
  300 CONTINUE
  100 CONTINUE
  200 CONTINUE
      END
```

Case II: Apple in Contact with Flat Surface

In this case the computer program uses Equation 5.2 and considers R_1 of the flat surface to be inifity and the modulus of elasticity of enamel steel as 206850 Mpa (30 x 10^6 Psi). Z for group I was determined to be 3.88 mm and the other groups were around 3.0 mm.

Computer Program for Calculation of Z in Case II, Group I :

```
      PROGRAM ORDER(INPUT,OUTPUT,TAPE5=INPUT,TAPE6=OUTPUT)
      DIMENSION E(150),EPS(150)
      READ(5,*)   (E(I),I=1,150),  (EPS(I), I=1,150)
      DO 200 N=80,150
      RN=N*1.0E-6
      PRINT 2,N
    2 FORMAT(*1N=*,I5)
      DO 100 I=1,1
      Y2=RANF(-1)
      I2=149.999*Y2+1
      E2=E(I2)        $    EPS2=EPS(I2)
      A=(RN*(1715277.769+6.5995*E2)/(8274000*E2))**(1./3.)
      P0=(.47746483*RN)/(A**(2.))
      DO 300 II=1,50
      Z=II*1.0E-4
      C=Z/A
      EPSMAX2=ABS((1./E2)*((1.35)*P0)*(.7*(1.-C*ATAN(1./C))-1./(1
     12.))))
      IF (EPSMAX2.LT.EPS2) GO TO 300
      PRINT 4,II,EPSMAX2
    4 FORMAT(*0II=*,I3,3X,*EPSMAX2=*,F10.3)
  300 CONTINUE
  100 CONTINUE
  200 CONTINUE
      END
```

APPENDIX E

LOADING OF CYLINDRICAL SPECIMENS AT DIFFERENT DEFORMATION RATES

APPENDIX E

LOADING OF CYLINDRICAL SPECIMENS AT DIFFERENT DEFORMATION RATES

To determine the effect of deformation rate on strain and stress at failure, a separate test was conducted. This time 20 apples were chosen and rates of deformation, 2.5 cm/min (1.0 in/min), 1.25 cm/min (0.5 in/min) and 0.5 cm/min (0.2 in/min) were used. The test was done on four different groups of apples. Group I were tested on October 1 (immediately after harvest), Group II were tested on November 15 (1.5 months of 2.2°C storage), Group III were tested on December 30 (3 months of 2.2°C storage), and Group IV were tested on Febaruary 15 (4.5 months of 2.2°C storage).

All apples which were stored at 2.2°C were removed from storage 24 hours prior to testing in order to get to the equilibrium with the laboratory temperature.

Table E1 gives the mean and standard deviation of stress and strain at failure for this test.

Table E1-- Compression test of apple tissue (Jonathan) at three different deformation rates

DEFORMATION RATE mm/min	STRAIN AT FAILURE				STRESS AT FAILURE (Kpa)				Secant Modulus of Elasticity (Kpa)			
	GROUP I	II	III	IV	I	II	III	IV	I	II	III	IV
25	0.15 (0.010)	0.12 (0.006)	0.13 (0.014)	0.12 (0.006)	450 (42)	250 (25)	240 (25)	215 (28)	3000 ( )	2083.33 ( )	1846.15 ( )	1791.6 ( )
12.5	0.15 (0.008)	0.12 (0.005)	0.13 (0.008)	0.12 (0.008)	440 (28)	240 (24)	230 (29)	210 (31)	2933.33 ( )	2000 ( )	1769.23 ( )	1750 ( )
5	0.15 (0.010)	0.12 (0.006)	0.13 (0.004)	0.12 (0.007)	430 (43)	230 (23)	220 (25)	200 (24)	2866.66 ( )	1916.66 ( )	1692.30 ( )	1666.6 ( )

Group I: Tested immediately after harvest. Group II: Tested with 1.5 months of storage (2.2°C) after harvest.

Group III: Tested with 3 months of storage (2.2°C) after harvest. Group IV: Tested with 4.5 months of storage (2.2°C) after harvest.

( ) Indicates Standard Deviation.

LIST OF REFERENCES

LIST OF REFERENCES

Apaclla, R.
1973 Stress analysis in agricultural products using finite element method. Unpublished technical research report. Agricultural Engineering Department, Michigan State University.

bittner, D. R., H. B. Manbeck and N. N. Mohsenin
1967 A method for evaluating cushing material used in mechanical harvesting and handling of fruits and vegetables. Transactions of ASAE, 10(6):711.

Boussineseq, J.
1885 Applications des potentiels a L'Etude de I'Equilibre et du Movement des Solids Elastiques, Paris.

Brown, R. L. and J. C. Richards
1970 Principles of powder mechanics, essays on the packing and flow of powders and bulk solids. Pergamon Press, London.

Burton, C. L. and B. R. Tennes
1977 Forced-air cooling of apples in a bulk storage. ASAE Paper No. 77-6512, St. Joseph, Michigan 49085.

Chappell, T. W. and D. D. Hamann
1968 Poisson's ratio and Young's modules for apple flesh under compressive loading. Transactions of the ASAE, 11(5):608-610.

Dal Fabbro, I. M.
1979 Strain failure of apple material. Unpublished Ph.D. dissertation, Michigan State University, East Lansing, Michigan.

Davis, R. A.
1974 A discrete probablistic model for mechanical response of a granular medium. Unpublished Ph.D. dissertation, Columbia University, New York, New York.

DeBaerdemaeker, J. G.
1975 Experimental and numerical techniques related to the stress analysis of apple under static load. Unpublished Ph.D. dissertation, Agricultural Engineering Department, Michigan State University.

Farouki, O. T. and H. F. Winterkorn
1964 Mechanical properties of granular system No. 52 National Research Council Highway Research Record.

Finney, E. E.
1963 The viscoelastic behavior of the potato, solanum Tuberosum, under quasi-static loading. Unpublished Ph.D. dissertation, Michigan State University, East Lansing, Michigan.

Fletcher, S. W., N. N. Mohsenin, J. R. Hammerle, and L. D. Turkey
1965 Mechanical behavior of fruits under fast rate loading. Transaction of the ASAE, 8(3):324-326, 331.

Fridley, R. B. and P. A. Adrian
1966 Mechanical properties of peaches, pears, apricots and apples. Transaction of the ASAE, 9(1):135-142.

Fridley, R. B., R. A. Bradley, L. W. Rumsey, and P. A. Adrian.
1968 Some aspects of elastic behavior of selected fruits. Transactions of the ASAE, 11(1):46-49.

Furnas, C. C.
1929 Flow of gases through beds of broken solids. U. S. Bureau of Mines Bulletin 307.

Gaston, H. P. and J. H. Levin
1951 How to reduce apple bruising. Michigan State University Agricultural Experimental Station Bulletin No. 374.

Graton, L. C. and H. J. Fraser
1935 Systematic packing of spheres with particulat relation to porosity and permeability. Journal of Geology, 43(8):785-909.

Gustafson, R. J.
1974 Continum theory for gas-solid-liquid media. Unpublished Ph.D. dissertation. Michigan State University, East Lansing, Michigan.

Hamann, D. D.
1967 Some dynamic mechanical properties of apple fruits and their use in the solution of an impacting contact problem of a spherical fruit. Unpublished Ph.D. dissertation. Virginia Polytechnic Institute, Blacksburg, Va.

Hamann, D. D.
1970 Analysis of stress during impact of fruit considered to be viscoelastic. Transactions of the ASAE, 13(6):893-899.

Hammerle, J. R. and N. N. Mohsenin
1966 Some dynamic aspect of fruits impacting hard and soft materials. Transaction of the ASAE, St. Joseph, Michigan 9(4):484.

Hertz, H.
1896 Miscellaneous papers. MacMillan and Company, New York, pp. 146-183; 261-265.

Horne, M. R.
1965 The behavior of an assembly of rotund, rigid, cohesion-less particles--Part I. Proceedings, Royal Society, London, England, Series A, Vol. 286, pp. 62-78.

Horsfield, B. C., R. B. Fridley and L. L. Claypool
1970 Application of theory of elasticity to the design of fruit harvesting and handling equipment for minimum bruising. ASAE Paper No. 70-811.

Horsfield, H. T.
1934 The strength of asphalt mixtures. Journ. Soc. Chem. Ind., 53:107T-115T.

Hudson, D. R.
1949 Density and packing in an aggregate of mixed spheres. Jour. Appl. Phys., 20:154-162.

Keck, H. and J. R. Goss
1965 Determining aerodynamic drag and terminal velocities of agronomic seeds in free fall. Transaction of the ASAE, 8(4):553-554, 557.

Marsal, R. J.
1963 Contact forces in solids and rockfill materials, Second Pan Am Conference on Soil Mechanics and Foundation Engineering, Vol. 2, pp. 67-98.

Mattus, G. E., L. E. Scott and L. L. Claypool
1960 Brown spot bruises of Bartlett pears, Proc. American Society of Horticultural Science, Vol. 75, pp. 100-105.

Miles, J. A. and G. E. Rehkugler
1971 The development of a failure criterion for apple flesh. ASAE Paper No. 71-652, St. Joseph, Michigan.

Mohsenin, N. N. and H. Göhlich
1962 Techniques for determination of mechanical properties of fruits and vegetables as related to design and development of harvesting and processing machinery. Journal of Agricultural Engineering Research 7(4):300-315.

Mohsenin, N. H., H. E. Cooper and L. D. Tukey
1963 Engineering approach to evaluating textural factors in fruits and vegetables. Transactions of the ASAE, 6(2):85-88.

Mohsenin, N. N., C. T. Morrow and L. D. Tukey
1965 The Yield-point nondestructive technique for predicting firmness of Golden delicious apples. Proc. of the Am. Soc. Hort. Sci. 86:70-80.

Mohsenin, N. N.
1971 Mechanical properties of fruits and vegetables review of a decade of research application and needs. ASAE Paper No. 71-849.

Morrow, C. T. and N. N. Mohsenin
1966 Consideration of selected agricultural products as viscoelastic materials. Journal of Food Science, 31(5):686-698.

Murase, H.
1977 Elastic stress-strain constitutive equations for vegetative material. Unpublished Ph.D. dissertation, Agricultural Engineering Department, Michigan State University.

Nelson, C. W. and N. N. Mohsenin
1968 Maximum allowable static and dynamic loads and effect of temperature for mechanical injury in apples. Journal of Agricultural Engineering Research,13(4):300-317.

Ross, I. J. and G. Isaac
1961 Forces acting in stack of granular materials (part I). Transaction of the ASAE,4(1):92.

Rumsey, T. R. and R. B. Fridely
1974 Analysis of viscoelastic contact stresses in agricultural products using a finite element method. ASAE, Paper No. 74-3513.

Sherif, S. M., L. J. Segerlind, and T. S. Frame
1974 An equation for the modulus of elasticity of radially compressed cylinder. Transactions of the ASAE (to be published).

Shigley, J. E.
1977 Mechanical Engineering Design, Third Edition. McGraw-Hill Series in Mechanical Engineering, New York, New York.

Shpolyaskaya, A. L.
1952 Structural mechanical properties of wheat grain. Colloid Journal (USSR) 14(1):137-148, Translated by Consultant Bureau, New York.

Slichter, C. S.
1899 Theoretical investigation of the motion of ground waters, U. S. Geol. Survey, 19th Ann. Report, Part 2, pp. 301-384.

Tennes, B. R., C. L. Burton and G. K. Brown
1978 A bulk handling and storing system for apples. Transaction of the ASAE, 6(21):1088-1091.

Timoshemko, S. P. and J. N. Goodier
1970 Theory of elasticity. McGraw-Hill Book Company, New York, New York.

Timbers, G. E., L. M. Staley, and E. L. Watson
1966 Some mechanical and rheological properties of the Netted Gem potato. Canadian Journal of Agricultural Engineering, February.